

Mineral equilibria at high PT-parameters

Khodorevskaya L.I., Kosova S.A., Safonov O.G., Viryus A.A. Experimental study of the graphite-mediated partial melting of two-mica schist at a pressure of 5 kbar and a temperature of 900 °C UDC 552.13

D.S. Korzhinskii Institute of Experimental Mineralogy RAS, Chernogolovka Moscow district. (khodorevskaya@mail.ru).

Abstract. The aim of our project was to study graphite-bearing protolith melting. The results of experiments on the partial melting of garnet-two-mica (with Qtz, Ap, Ilm) schist containing 4 mas.% H₂O in the presence of 0-20 mas. % graphite at a pressure of 5 kbar and a temperature of 900°C, are reported. The mineral associations of samples after the experiments include quartz, garnet, apatite, ilmenite and the newly-formed products of peritectic reactions, such as melt, K-feldspar, spinel, gedrite and sillimanite. Fe³⁺/(Fe³⁺+Fe²⁺) ratio in Fe-Mg minerals (ilmenite, spinel and gedrite) decreases with an increase in graphite abundance, indicating more intensive reducing conditions. Preliminary data also show that more reducing conditions (when graphite is more abundant) contribute to a higher Na/K ratio in melts.

Keywords: garnet-two-mica metapelite; dehydration melting; graphite; granitoid melts; fluids.

Graphite is the most important constituent of metamorphic (mainly metasedimentary) rocks in continental crust domains where metamorphism and granite formation take place. Its oxidation during metamorphic reactions, including partial melting, is often interpreted as a possible “internal” source of CO₂, a typical component of fluids under high-temperature metamorphic conditions. The transformation of graphite into CO₂ at T-P parameters is dependent on f_{O_2} . In the absence of external buffering, oxidation-reduction conditions are controlled by H₂O concentration in the system and/or the abundance of Fe³⁺ concentrated mainly by mica in metasedimentary rocks.

The aim of our project was to study garnet-two-mica (with Qtz, Ap, Ilm) schist melting, depending on the variable concentrations of C-O-H components in fluid, when the system is saturated with carbon in the form of graphite. In the system studied, fluid phase composition is controlled by H₂O, which is formed upon biotite and muscovite decomposition, and variable graphite concentration.

The experiments were conducted using an ampoule technique on high gas pressure installations at a temperature of 900°C and a pressure of 5 kbar. 25–40 mg of schist, mixed thoroughly with graphite, were placed into a 10-12 mm high vertically standing ampoule, 3 mm in diameter. The schist sample consisted of muscovite (43%), quartz (30%), biotite (13%), garnet (10%), ~1.5% apatite and ~1.5%

ilmenite (the mineral and chemical compositions of the rock are shown in Mityaev et al., 2022). The amount of the graphite added made up 0 to 20% of schist sample mass. The smallest amount of graphite in the system made up 4% of the sample, i.e., fluid composition was formed under graphite + fluid equilibrium conditions (Danilov, 2005). The ampoules were welded up by PUK-04 electrical argon-arc welding and were kept for 7 days in an experimental regime. Oxygen volatility in the experiments was not controlled, assuming that this parameter was buffered by phase associations. After the experiments, the ampoule was opened, the solid sample extracted was placed into a container, covered with epoxy resin, polished and analyzed. Mineral phase compositions were studied by electron probe X-ray microanalysis on Tescan VEGA TS 5130MM and VEGA-II XMU scanning electron microscopes equipped with INCAx-sight energy-dispersive X-ray spectrometers. These operations were performed at an accelerating voltage of 20 kV, a beam current of 150–250 pA and a spectrum formation time of 70 s for various phases. The melts formed during the experiments were analyzed at points (excitation area was up to 5 μm in diameter) and sites covering an area of 10 × 10–20 × 20 μm. As a rule, analytical results coincided.

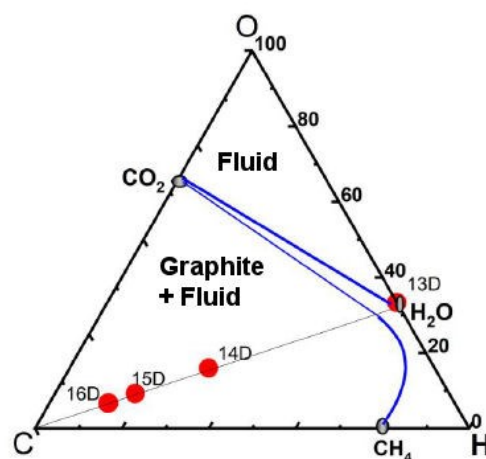


Fig. 1. C-O-H diagram with a saturation surface isotherm at 900°C and 5 kbar (Danilov, 2005). Circles indicate the composition of original fluid in the experiments.

In the composition triangle of the fluid C-O-H (Fig.1), the convex line indicates the graphite saturation surface of the system and separates two composition domains: two-phase and one-phase, in which fluid with graphite and homogeneous fluid are in stable equilibrium. The boundary separating the

domains is a carbon saturation level for the above temperature and pressure values. The composition of the fluid equilibrated with graphite corresponds to the point on the saturation line formed upon its intersection by a straight line extending from angle C across the composition of system. Correspondingly, all compositions from the two-phase domain displaying the same O/H ratio would have the same equilibrated fluid composition (Danilov, 2005). Our experiments with graphite are all in the two-phase fluid field (Fig.1). Fluid phase composition in our experiments lies on the straight line C-H₂O (O/H=1/2), where experiment 13D indicates fluid composition in the absence of graphite in the system. Calculated data (Danilov, 2005) show that at 900°C and 5 kbar the fluid has the following composition: X_{H₂O} = 0.66, X_{CO₂} = 0.14, X_{CH₄} = 0.14,

X_{CO} = 0.03, X_{H₂} = 0.02, and variations in graphite concentration in the original mixture do not affect equilibrated fluid composition. However, they are responsible for the activity of water and, correspondingly, f_{O₂}, in accordance with the equilibrium H₂ + 1/2O₂ = H₂O. In our experiments, a Fe²⁺/Fe³⁺ ratio in spinels, ilmenites and orthoamphiboles is the most accessible indicator of O₂ fugacity.

Results of experiments

Quartz, garnet, apatite and ilmenite from original metapelite persist after the experiments, while biotite and muscovite are absent. Hercynitic-magnetitic spinel (Hc), melt (Gl), sillimanite (Sill), K-feldspar (Kfs) and orthoamphiboles (oHbl) are newly-formed phases.

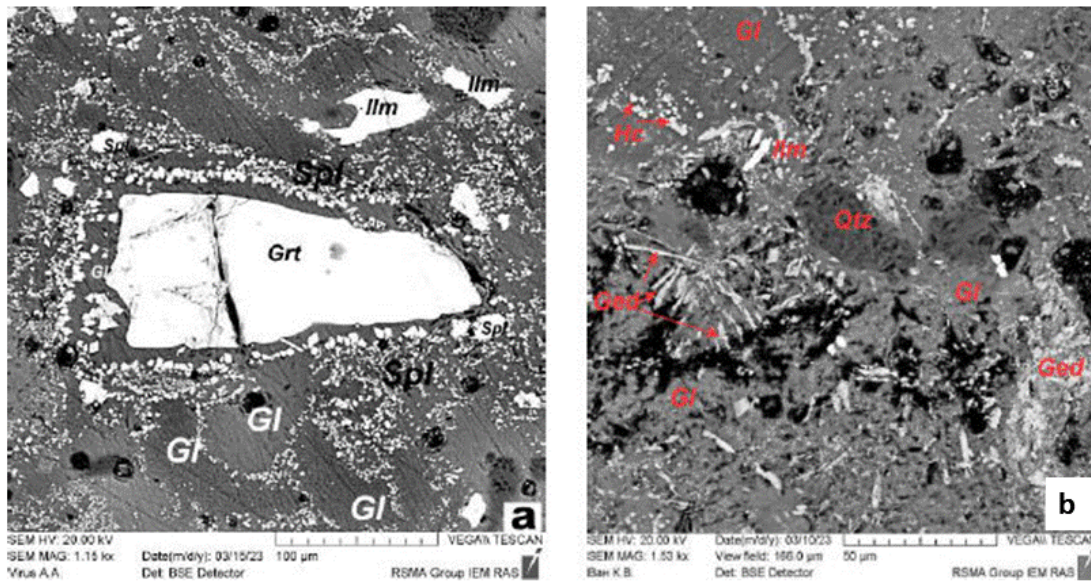


Fig. 2. Experimental products in back-scattered electrons (BSE): a - hercynitic-magnetitic spinel chains around garnet, Gl, Ilm, Q (experiment 14D, 4 mas. % of graphite); b - acicular and prismatic gedrite crystals among melt hardening products Gl, Q (experiment 16D, 20 mas.% of graphite).

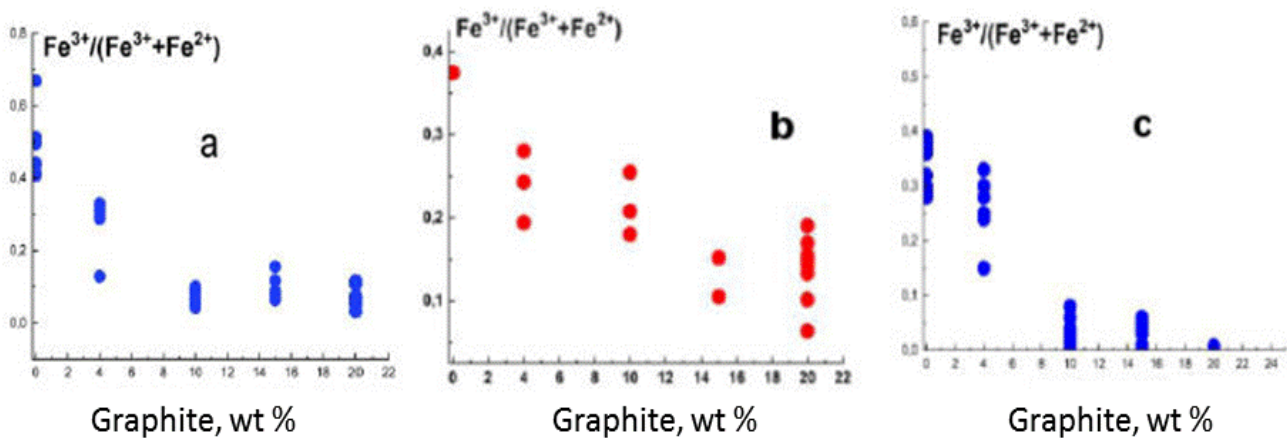


Fig. 3. Variations in a Fe³⁺/(Fe³⁺+Fe²⁺) ratio in ilmenite (a), orthoamphibole (b) and spinel (c) with an increase in graphite concentration.

Hercynitic-magnetitic spinel forms chains around almandine garnet at its contact with melt (Fig. 2a). In graphite-free experimental products, scarce Kfs laminae and acicular Sill crystals measuring up to 20 μm are trapped in glass. As graphite concentration increases, Sill crystals decrease markedly in size. Fine elongated amphibole (oHbl) crystals, similar in composition to gedrite $\text{Na}_x(\text{Mg}, \text{Fe}^{2+}, \text{Mn})_{7-y} \text{Al}_y(\text{Si}_{8-x-y} \text{Al}_{x+y} \text{O}_{22})(\text{OH}, \text{F}, \text{Cl})_2$, are scarce in graphite-free experiments (1-2 grains), but their amount in experiments with 20% graphite increases considerably (Fig. 2b).

As graphite concentration increases in original mixtures in all Fe-Mg minerals, $\text{Fe}^{3+}/(\text{Fe}^{3+}+\text{Fe}^{2+})$ ratio decreases (Fig. 3a-c).

Thus, a decrease in the $\text{Fe}^{3+}/(\text{Fe}^{3+}+\text{Fe}^{2+})$ ratio of Fe-bearing minerals proves that an increase in graphite concentration in the system results in more intensive reducing conditions, making it possible to analyze melt compositions, depending on f_{O_2} regime.

Mityaev et al. (2022) have shown that garnet-two-mica metapelite begins to melt at 750 - 800°C. Our experiments carried out at 900°C and at a similar pressure indicate that the partial melting of the schist

was provoked by peritectic reactions, in which biotite and muscovite were involved and ~50-60 % melt was formed. The melt contains 70-74 mas. % SiO_2 and 13-16 mas. % Al_2O_3 (recalculated per anhydrous residue). The ratio $\text{FeO}/(\text{FeO} + \text{MgO}) = 0.8 - 0.9$ remains almost unaffected by variations in graphite concentration in the system. The ratio values are similar because at preset parameters melt formation was controlled only by the reaction $\text{Bt} + \text{Ms} + \text{Qz} \rightarrow \text{melt} + \text{Kfs} + \text{Spl} + \text{oHbl} + \text{Sill}$ at all graphite concentrations. The formation of the same Fe-Mg minerals (spinel, gedrite), as well as ilmenite present in the original sample, concentrate the bulk of Fe и Mg, controlling the abundances of these elements in melts.

The index $\text{MALI} = (\text{K}_2\text{O} + \text{Na}_2\text{O}) - \text{CaO}$ (Frost et al., 2001) increases on the average from 7 to 14 with an increase in graphite concentration, because CaO concentration in the melt is controlled by the involvement of apatite in melting reactions. In the absence of graphite, apatite contributes to melting, while increased graphite concentration does not contribute to apatite melting, so CaO concentration in the melts decrease, increasing the MALI index.

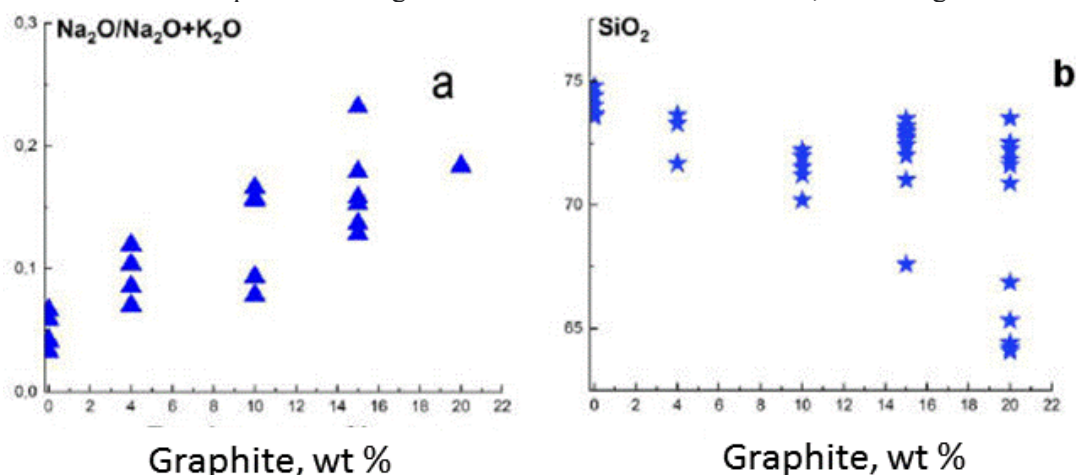


Fig. 4. Variations in $\text{Na}_2\text{O}/(\text{Na}_2\text{O}+\text{K}_2\text{O})$ (a) and SiO_2 (b) (mas.%) provoked by changes in graphite concentration.

Figure 4 shows how the ratio $\text{Na}_2\text{O}/(\text{Na}_2\text{O}+\text{K}_2\text{O})$ (a) and SiO_2 (b) varies in the melts with various graphite concentrations in the experiments. It can be seen that as reducing conditions become more intensive, the melts contain more sodium. The decrease of f_{O_2} , provoked by increasing graphite concentration in the experiments, seems to make K-feldspar more stable relative to the melt. The SiO_2 content of the melts varies from 70 to 75 mas.%, decreasing slightly with the growth of graphite concentration in the system. This could be due to the fact that as graphite in the system becomes more abundant, the concentration of carbonaceous components in the melt, such as molecular CO_2 and/or CO_3^{2-} group, increases, triggering the partial polymerization of an alumosilicate network by

forming complexes with cation-modifiers (Mysen et al., 1982). This effect correlates with an increase in a $\text{Na}_2\text{O}/(\text{Na}_2\text{O}+\text{K}_2\text{O})$ ratio, coinciding with the positive effect of Na_2O and total alkalinity on the solubility of CO_2 in silicate melts (e.g., Ni, Keppler, 2013).

Funding. This work was supported by a state contract of IEM RAS (FMUF-2022-0004).

References

- Danilov B. S. Physico-chemical modelling of the effect of fluid regime on the metamorphism of basic rocks. Diss. Cand. Geol.-Min. Sci. 2005. Irkutsk: RAS. Institute of the Earth's Crust. 145 p.
Mityaev A.S., Safonov O.G., Varlamov D.A., Van Reenen D.D., Serdyuk A.A., Aranovich L.Y. Partial Melting

of Plagioclase-Free Garnet-Two-Mica Metapelite as a Model of the Formation of Ultra-K Felsic Magmas in the Continental Crust // *Doklady Earth Sciences*. 2022. V. 507. № 2. P. 253-261.

Frost B.R., Barnes C.G., Collins W.J. et al. A geochemical classification for granitic rocks // *J. Petrol.* 2001. V. 42. P. 2033–2048.

Mysen B. O., Virgo D., Seifert F. A. The structure of silicate melts: implications for chemical and physical properties of natural magma // *Reviews of Geophysics*. – 1982. T. 20. №. 3. C. 353-383.

Ni H., Keppler H. Carbon in silicate melts // *Reviews in Mineralogy and Geochemistry*, V. 75, P. 251-287

Kuzyura A.V., Litvin Yu.A., Spivak A.V. Peritectic reaction of olivine in diamond forming system carbonate – silicate - (C-O-H)-fluid at 6 GPa UDC 123.456

Korzhinskii Institute of Experimental Mineralogy RAS
shushkanova@iem.ac.ru

Abstract. The influence of the components of the supercritical C-O-H-fluid (at a content of 7.5 wt. %) on the phase relations during melting of the multicomponent diamond-forming system olivine-jadeite-diopside-(Mg-Fe-Ca-Na-carbonates) - (C-O-H) was revealed Experimentally at 6 GPa and 700 – 1200 °C (conditions of the upper mantle). The peritectic reaction of olivine and jadeite-bearing melt with the formation of garnet has been established as the key mechanism of the ultrabasic-basic evolution of diamond-forming melts. The supercritical C-O-H-fluid during the melting of the multicomponent diamond-forming system olivine – jadeite – diopside - (Mg-Fe-Ca-Na-carbonates) - (C-O-H) in the experiment has a significant effect on the phase relations. Its CO₂-component as a metasomatic agent is actively involved in the surplus carbonatization of silicate solid phases and melts of diamond-forming media. The H₂O-component of the fluid, together with carbonate compounds of the diamond-forming system, significantly decreases the temperature of the liquidus and solidus boundaries, including the temperature of the established peritectic reaction of olivine and jadeite-bearing melt. After crystallization of a completely miscible silicate-carbonate-fluid melt is finished, a supercritical aqueous fluid phase and hydrous carbonate nesquegonite MgCO₃×3H₂O was found in the subsolidus of the diamond-forming system. It was identified by Raman spectroscopy.

Keywords: *diamond-forming system, upper mantle, C-O-H fluid, ultrabasic-basic evolution, silicate-carbonate-fluid, peritectic reactions, supercritical hydrothermal system*

In accordance with the mantle-carbonatite theory of genesis of diamond and associated phases (Litvin, 2017), diamond growth media were formed under the influence of large ascending flows of supercritical C-O-H fluids. CO₂ metasomatism of primary mantle silicate minerals was carried out by these flows with the formation of Mg, Fe, Ca, Na carbonates and their melts. Chambers of multicomponent silicate-carbonate matter arose within the silicate rocks of the

upper mantle. Their volumes increased as a result of CO₂-carbonatization of silicates, as well as the dissolution of mantle minerals in the formed carbonate melts and then in completely miscible silicate-carbonate ones. When the temperature of the diamond-forming chamber decreases, silicate-carbonate-carbon solutions-melts supersaturated to diamond appear, which ensures its spontaneous crystallization. As a result, both diamonds with paragenic inclusions of associated minerals and diamondiferous peridotites and eclogites are formed. The supercritical fluid components CO₂ and H₂O were dissolved in the growth silicate-carbonate melts and were captured by the growing diamonds. Diamond-bearing rocks and diamonds with inclusions were transported from the upper mantle by kimberlite magmas to the Earth's crust along with xenoliths of peridotite and eclogite rocks hosting for the mantle diamond-forming chambers (Dawson, 1980; Marakushev, 1984).

The study of xenoliths of diamondiferous peridotites and eclogites in kimberlites (Litvin et al., 2020), as well as paragenic inclusions of peridotite and eclogite minerals in diamonds from kimberlite deposits (Sobolev, 1974) suggested the probability of ultrabasic-basic evolution of diamond-forming melts at the depths of the upper mantle. The study of the course of geochemical reactions leading to such an evolution can only be solved with the help of experimental modeling in combination with theoretical physico-geochemical methods for studying phase equilibria.

It has been experimentally demonstrated that evolution of the upper mantle ultrabasic magmas should be controlled by the peritectic reaction of orthopyroxene and melt with the formation of clinopyroxene (Litvin, 1991; Litvin et al., 2016). At the same time, a critically important boundary change in the compositions of the upper mantle melts from ultrabasic to basic is provided by the peritectic reaction of olivine and jadeite-bearing melt with the formation of garnet in the experiment without the participation of fluid components (Litvin et al., 2019).

The role of supercritical C-O-H-fluid (with a content of 5.0 wt %) at the fractional ultrabasic-basic evolution of melts of the upper mantle silicate system olivine-jadeite-diopside-(C-O-H) was investigated (Litvin, Kuzyura, 2021). It was found that the CO₂ component of the fluid is almost completely consumed by metasomatic carbonatization of the upper mantle derivative minerals. As a result, many small grains of Mg, Fe, Ca, and Na carbonates were identified among the experimental products. Impurity carbonates are formed at the action of CO₂ on silicate minerals, they are assimilated by completely miscible silicate-carbonate melts, while the H₂O component is

dissolved in completely miscible silicate-carbonate melts.

The purpose of this work is to model the physicochemical possibility of ultrabasic-basic evolution of the mantle diamond-forming substance and studying the effect of C-O-H fluid on the process.

The tasks of the work were:

1. Experimental studies at 6 GPa of the effect of supercritical C-O-H-fluid (at its increased content of 7.5 wt. %) on phase melting relations of the multicomponent diamond-forming system olivine - jadeite - diopside - (Mg-Fe-Ca-Na-carbonates) - (C-O-H-fluid).

2. Estimation of the reactivity of the supercritical H₂O fluid as a hydrothermal component in the subsolidus mineral association of the studied diamond-forming system.

In this work, experimental studies of the phase melting relations of a model mantle diamond-forming carbonate-silicate-fluid system olivine Ol [(Mg,Fe)₂SiO₄] - jadeite Jd [NaAlSi₂O₆] - diopside Di [CaMgSi₂O₆] - Mg-Fe-Ca-Na-carbonates - C-O-H-fluid was performed at pressure 6 GPa and in the

temperature range of 700-1200 °C with using of anvil-with-hole toroidal type apparatus at the IEM RAS. The source of the fluid is oxalic acid dihydrate, which decomposed in the experiments to form CO₂, H₂O. The quenched samples were studied using scanning electron microscopy and X-ray microanalysis CamScanMV230 (VEGA TS 5130MM) with a Link INA Energy-350 energy-dispersive analyzer (accelerating voltage 20 kV); 2500i with a Pixis2K CCD detector cooled to -70°C and an Olympus microscope with a solid-state single-mode laser with a wavelength of 532 nm.

Based on the results of the experiments, a phase diagram of the polythermal section Ol₇₄Carb_{18.5}(C-O-H)_{7.5} - Omp₇₄Carb_{18.5}(C-O-H)_{7.5} was plotted (Fig. 1). The position of the peritectic point P at 64 wt. % of the boundary Ol-bearing component of the polythermal section and 1000–1020 °C is determined by the combined influence of (C-O-H)-fluid and the carbonate component of the diamond-forming system. Olivine is effectively soluble in the carbonate-silicate melt, which activates its peritectic reaction with the jadeite component.

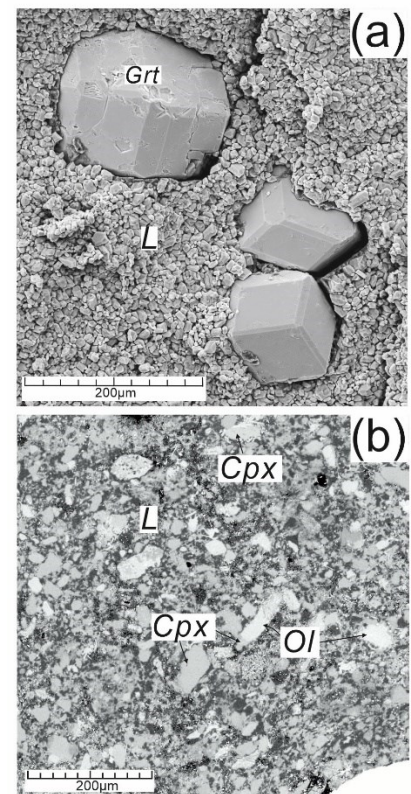
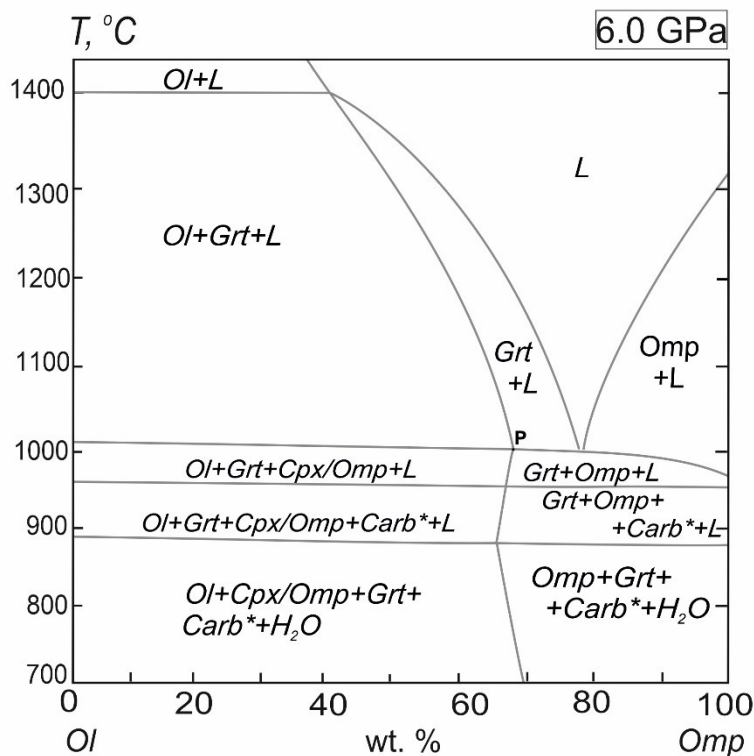


Fig. 1. Experimental melting phase relations in polythermal section Ol₇₄Carb_{18.5}(C-O-H)_{7.5} - Omp₇₄Carb_{18.5}(C-O-H)_{7.5} of ultrabasic-basic diamond-forming system Ol-Jd-Di-(C-O-H). P – peritectic point

Fig. 2. SEM-photo of experimental samples: a) Ultrabasic association: Smp1 3292, [(Ol₈₀Omp₂₀)₈₀Carb₂₀]_{92.5}COH_{7.5}, 930 °C, duration 120 min; b) Basic association: Smp1. 3326 [(Ol₄₀Omp₆₀)₈₀Carb₂₀]_{92.5}COH_{7.5}, 950 °C, duration 90 min

Experiments shows that the peritectic reaction takes place in the silicate-carbonate-fluid diamond-forming system, ultrabasic (Ol+Cpx/Omp+Carb+L)

association is formed on the solidus, then it transits to the basic (Grt+Omp+Carb+L) association (Fig. 2). The average composition of the resulting olivine

corresponds to $(\text{Mg}_{0.58}\text{Fe}_{0.42})_2\text{SiO}_4$. The compositions of clinopyroxene/omphacite are characterized by the content of the jadeite component $\text{NaAlSi}_2\text{O}_6$ in the range of 10 - 67 wt. %. Garnets have grossular-pyrope compositions with a variation in the content of the pyrope component in the range of 10–46 wt. %. Garnets are characterized by spontaneous nucleation, their sizes reach 200 microns (Fig. 2a). Garnets are products of the peritectic reaction (P) of olivine with a jadeite-bearing completely miscible silicate-carbonate melt with a dissolved supercritical aqueous fluid.

At the experimental conditions, the reactive activity of the supercritical fluid H_2O solution as a hydrothermal component in the subsolidus of the Ol-Jd-Di-(reactive Grt)- MgCO_3 - FeCO_3 - CaCO_3 - Na_2CO_3 - (C-O-H-fluid) diamond-forming system manifests itself. Localized water reservoirs and geodes can be formed, which are found in hermetic Pt ampoules after they are opened at normal pressure and temperatures (Fig. 3a). Probably, they appeared as accumulations of supercritical H_2O fluids among silicate-carbonate substance at the PT-conditions of the experiment.

The use of Raman spectroscopy in the analysis of

the substance that fills such structures made it possible to identify the hydrous carbonate mineral, nesquehonite (Nes) $\text{MgCO}_3 \cdot 3\text{H}_2\text{O}$ among common carbonates and silicates, both individually and as a paragenic inclusion in garnet (Fig. 3b).

Thus, the possibility of ultrabasic-basic evolution of diamond-forming fluid-bearing melts has been experimentally demonstrated in the study. Supercritical C-O-H-fluid (at a content of 7.5 wt.%) has a significant effect on the phase melting relations of the multicomponent diamond-forming system olivine - jadeite - diopside - (Mg-Fe-Ca-Na-carbonates) - (C-O- H) in the experiment at 6 GPa and 700 - 1400 °C. Its component CO_2 as a metasomatic agent is actively involved in the additional carbonatization of silicate solid phases and melts of diamond-forming media. In this case the supercritical fluid H_2O dissolved in carbonate-silicate melts significantly lowers their melting temperatures, including the temperature of the peritectic reaction of olivine and jadeite-bearing melt. At the same time, the H_2O supercritical fluid is a physicochemical factor in activation of hydrothermal processes, which minerals of the subsolidus association of the the upper mantle diamond-forming systems involve in.

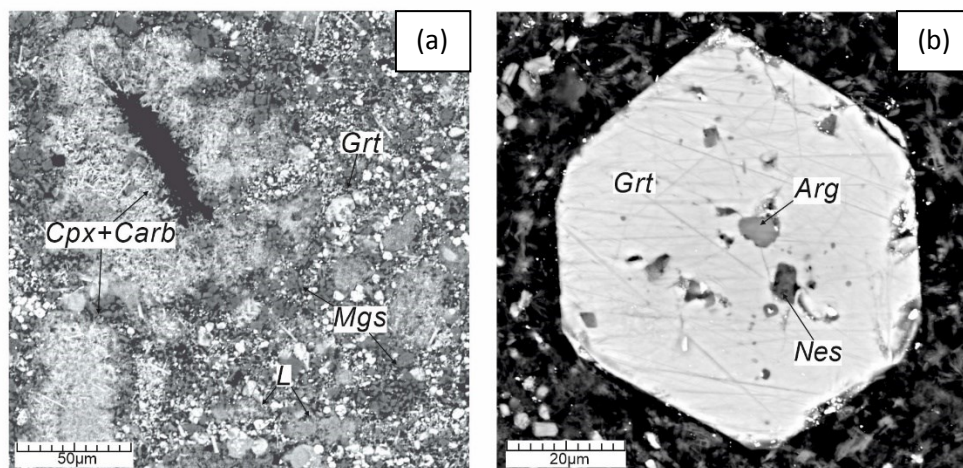


Fig. 3. SEM-photo of experimental samples showing reactive activity of supercritical fluid H_2O -solution: a) Smp1 № 3291, $[(\text{Ol}_{80}\text{Omp}_{20})_{80}\text{Carb}_{20}]_{92.5}\text{COH}_{7.5}$, 1020 °C, duration 95 min. With geodes; b) Smp1 № 3309, $[(\text{Ol}_{30}\text{Omp}_{70})_{80}\text{Carb}_{20}]_{92.5}\text{COH}_{7.5}$, 950 °C, 90 min. With nesquehonite

This study is fulfilled under Research program № FMUF-2022-0001 of the Korzhinskii Institute of Experimental Mineralogy.

References:

Sobolev N. V. Deep-seated inclusions in kimberlites and the problem of the composition of the upper mantle. – American Geophysical Union, 1977
 Litvin Yu. A. Physicochemical studies of the melting of the deep-seated matter of the Earth. Moscow: Science, 1997 (in Russian)
 Litvin Y. A., Kuzyura A. V. (2021) Peritectic reaction of olivine in the olivine–jadeite–diopside–garnet–(C-O-H) system at 6 gpa as the key mechanism of the

magmatic evolution in the upper mantle. *Geochemistry International*. V. 59. 9. P. 813–839.
 Litvin Yu. A., Kuzyura A. V., Bovkun A. V., Varlamov D. A., Limanov E. V., Garanin V. K. (2020) Genesis of diamondiferous rocks from upper-mantle xenoliths in kimberlite. *Geochem. Int.* 58(3), 245-270.
 Litvin Yu. A., Kuzyura A. V., Limanov E. V. The role of garnetization of olivine in the olivine–diopside–jadeite system in the ultramafic–mafic evolution of upper-mantle magmatism (experiment at 6 GPa) // *Geochemistry*. -2019. -V. 57. -P. 1045-1065.
 Litvin Yu. A., Spivak A. V., Kuzyura A. V. Foundations of the mantle-carbonatite concept of diamond genesis // *Geochemistry International*. –2016. -V. 54. -№ 10. - P. 839-857.

- Marakushev A. A. Peridotite nodules in kimberlites as indicators of the deep structure of the lithosphere / Reports of Soviet geologists at the XXVII session of the International Geological Congress. Petrology. – 1984. - P. 153-160 (in Russian)
- Dawson J.B. (1980) Kimberlites and their Xenoliths. Berlin, Springer-Verlag. Xii+252 p.
- Litvin Yu.A. (2017) Diamonds and Associated Phases. Springer Mineralogy, 137 p.

Chertkova N.V.¹, Spivak A.V.¹, Burova A.I.², Litvin Yu.A.¹, Zakharchenko E.S.¹, Kuzyura A.V.¹, Bovkun A.V.², Safonov O.G.^{1,2}, Bobrov A.V.^{1,2,3} Experimental investigation of stability fields for water-bearing minerals in the FeTiO₃-Mg₂SiO₄-H₂O system at 6 GPa

¹D.S. Korzhinskii Institute of Experimental Mineralogy RAS, Chernogolovka; ²Lomonosov Moscow State University, Moscow; ³Vernadsky Institute of Geochemistry and Analytical Chemistry RAS, Moscow; e-mail: nadezda@iem.ac.ru

Abstract. Experimental data describing stability of hydrous minerals at high pressures contribute to our understanding of the processes of volatile transport to the mantle depths and are necessary for geodynamic modeling. This work presents results of the experiments studying phase relations in the FeTiO₃-Mg₂SiO₄-H₂O system at 1200-1250 °C and 6 GPa, using natural minerals and chemical reagents as starting materials. Analysis of the observed water-bearing phases was carried out with the evaluation of the factors that influence the expansion of their stability fields to the region of high temperatures.

Key words: upper mantle, experiment, high pressures, hydrous fluid, phase relations, humite group minerals

The presence of even a small amount of water in

Table 1. Conditions and results of experiments with excess water in the system.

Starting composition	T, °C	P, GPa	Run products
Natural system Ilm-Ol-H₂O			
Ilm ₅₀ Ol ₅₀ + H ₂ O	1200	6	Ilm, Ol, Px, Hum
Model system Ilm-Ol-H₂O			
Ilm ₇₅ Ol ₂₅ + H ₂ O	1250	6	Ilm, Ol
Ilm ₅₀ Ol ₅₀ + H ₂ O	1250	6	Ilm, Px, Hum
Ilm ₂₅ Ol ₇₅ + H ₂ O	1250	6	Ilm, Px, Hum

Notes: Ilm – ilmenite, Ol – olivine, Px – pyroxene, Hum – humite-group minerals.

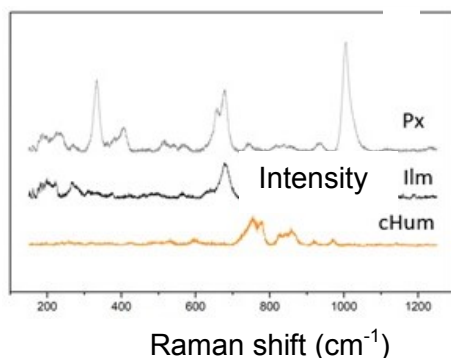


Fig. 1. Raman spectra of run products in the model system Ilm₅₀Ol₅₀ + H₂O.

the system affects the phase relationships, melting points and rheological properties of mantle rocks, therefore, works studying the phase relationships and stability of hydrous minerals at high pressures and temperatures are important for understanding the processes, which take place at the conditions corresponding to the Earth's upper mantle.

The objective of this work was to study the stability fields of the humite-group minerals in the FeTiO₃-Mg₂SiO₄-H₂O system under the *P-T* conditions of the Earth's upper mantle.

In two series of experiments, both natural minerals (ilmenite and olivine) and mixtures of chemical reagents in appropriate stoichiometric proportions with the addition of distilled water, were used as starting materials. The experiments were carried out employing the Bridgeman-type apparatus with a toroidal seal at the pressure of 6 GPa, temperatures of 1200–1250°C and run duration of 60 min. Gold capsules, filled with starting mixtures and sealed along the perimeter, were placed in the high-pressure cell. After quenching, the experimental products were studied using micro X-ray spectral analysis and Raman spectroscopy.

According to the experimental results (Table 1), OH-containing silicate phases in the studied systems are represented by minerals of the humite group with the general formula M_{2n}Si_nO_{4n}•M(OH)₂ (M = Mg, Fe, Ti). Humite-group minerals were detected in experiments with a high content of the olivine component in the starting composition.

Raman spectroscopy analysis confirmed the presence of clinohumite (cHum) in the experimental products (Figure 1).

Micro X-ray spectral analysis showed that the minerals of the humite group obtained in the

experiments contain up to 7.27 wt. % TiO₂ (Table 2).

Table 2. Average compositions of phases synthesized in the Ilm-Ol-H₂O model system at 6 GPa and 1250 °C.

Starting composition	Ilm ₇₅ Ol ₂₅ + H ₂ O		Ilm ₅₀ Ol ₅₀ + H ₂ O			Ilm ₂₅ Ol ₇₅ + H ₂ O		
Phase	Ilm	Ol	Ilm	Px	Hum	Ilm	Px	Hum
SiO ₂	н.п.о.	26.44	н.п.о.	48.49	28.04	н.п.о.	55.63	32.06
TiO ₂	55.75	1.41	52.73	1.80	5.88	57.58	2.02	7.27
MgO	6.29	27.93	5.00	24.18	32.31	9.24	35.52	40.78
FeO	37.42	31.27	42.16	16.81	29.00	32.66	7.35	12.08
Total	99.47	87.05	99.88	91.27	95.22	99.39	100.52	92.2

Previous experimental studies have shown that OH-bearing humite-group minerals are stable at high pressures, but break down at temperatures above 1150 °C (e.g., Yamamoto and Akimoto, 1977; Stalder and Ulmer, 2001). High contents of Ti and Fe in the synthesized samples can expand their stability fields to the region of low pressures and high temperatures. Another factor that can influence the expansion of the stability fields of humite-group minerals to higher temperatures is the excess of water in the experiments performed in this work. The stability of humite-group minerals under conditions corresponding to the upper mantle contributes to the understanding of volatile recycling processes.

complexes – in the Maksyutov eclogite-glaucophane schist complex (Southern Urals) and in the Atbashi unite (Southern Tien Shan). Thermobaric processes in these terranes determine changes in the PT parameters of metamorphism, and lead to the formation of contrasting series of rocks. Such series are formed as a result of tectonic intrusion (mélange) of high-pressure eclogite inclusions (individual blocks, boudins, interlayers and lenses) into the thickness of a weakly metamorphosed host matrix and their further joint (coherent) development. At the regressive stage of development of the complexes, the processes of the petrochemical (metasomatic) direction join the thermobaric processes, as a result of which the bulk chemical composition of the rocks changes. The first article from couple cycle deals with materials on the relatively deep Maksyutov complex. The second paper presents the results of the study of the Atbashi complex formed at moderate pressure.

Acknowledgments: This work was carried out with the support of the Russian Science Foundation (project No. 20-77-00079) and partially within the Research program FMUF-2022-0001 of the Korzhinski Institute of Experimental Mineralogy RAS

Keywords: high-pressure metamorphism, thermobaric processes, petrochemical alterations, Maksyutov complex, Atbashi complex, tectonic mélange, coherent processes, PT path in metamorphism evolution.

References

1. Stalder R., Ulmer P. (2001) Phase relations of a serpentine composition between 5 and 14 GPa: Significance of clinohumite and phase E as water carriers into the transition zone // Contributions to Mineralogy and Petrology, V. 140, P. 670–679.
2. Yamamoto K., Akimoto S.-I. (1977) The system MgO-SiO₂-H₂O at high pressures and temperatures; stability field for hydroxyl-chondrodite, hydroxylclinohumite and 10 Å-phase // American Journal of Science, V. 277, P. 288–312.

Fedkin V.V. Combined processes of eclogite-glaucophane schist formation: I. Maksyutov complex, Southern Ural UDC 549.6+552.16:552.48

D.S. Korzhinski Institute of Experimental Mineralogy
Russian Academy of Sciences vfedkin@iem.ac.ru

Abstract. The interconnected combined processes of metamorphic and metasomatic evolution of crustal mafic eclogites are considered in two high-pressure metamorphic

It is known that classical (isochemical) metamorphism is almost always accompanied by metasomatism, fluid action, which results in chemical changes in rock composition, mineral reactions, processes of dissolution and redeposition of chemical components. In fact, the real final picture of the metamorphic complex, its final appearance and state is formed by a combination of coherent (compatible) metamorphic and metasomatic processes. Thermobaric (metamorphic) processes determine the RT parameters of mineral equilibria and the general level of metamorphism, while petrochemical processes cause metasomatic changes in the bulk chemical composition of rocks. This paper considers the interrelated processes of metamorphic and metasomatic evolution of crustal mafic eclogites, which are formed in the junction zones of large geosstructural elements of the Earth's crust under conditions of constant tectonic activity, a changing metamorphism regime, and a fairly high mobility of fluid flows (Dobretsov and Sobolev, 1977; Sobolev, Shatsky, 1986; Dobretsov et al., 1996). In this regard, the processes of metasomatism

and metamorphic transformations are closely related and determine the final outcome of the development of the complex. The problem is solved by the methods of phase correspondence matching and mineralogical thermobarometry based on the Grt¹-Cpx-Pl-Qz equilibrium - the main information source of the conditions for the formation of HP rocks.

Well-known well-studied eclogite-glaucophane schist complexes were chosen as the object of study: the Maksyutov complex in the Southern Urals and the Atbashi complex in the Southern Tien Shan. Both complexes are part of the system of the intracontinental Ural-Mongolian Hercynian foldbelt. Both complexes, located in the collision zone of the junction of the continental margin and the pale ocean, have a similar lithological structure. The lower high-pressure part of the section represents the marginal parts of the continental plates in the form of a mafic eclogite member. The upper, ophiolite-like sequence is part of the pale oceanic crust with fragments of continental clasts (Dobretsov et al., 1996). The complexes have close temperature and age intervals, but differ in the pressure level of their formation. The relatively deep Maksyutov complex was formed in the rift zone in the diamond and coesite stability field at T=700-750°C and P=3.0-3.2 GPa (Lennykh, et al., 1995; Dobretsov et al., 1996; Beane, Leech, 2007). The Atbashi terrane of moderate pressure traces the most important tectonic boundary between the Middle and Southern Tien Shan. It was formed in an island-arc setting, in the area of stability of the Ab-Jd-Qz parageneses at T=650-700 °C and P=1.2-1.4 GPa (Fedkin, 2004). Differences in the formation conditions of these complexes make it possible to identify and compare the possible features of the course of joint metamorphic and metasomatic processes of their development.

The problems of metamorphism of the Maksyutov Complex have been discussed in the literature for decades (Chesnokov and Popov, 1965; Lennykh, et al., 1995; Dobretsov et al., 1996; Beane and Leech, 2007), and the thermobaric history of its development has been described in sufficient detail. The last data obtained (Valizer et al., 2013; Fedkin, 2020, Fedkin et al., 2021) confirm the maximum parameters of the initial stage of metamorphism: T=800→900°C - at the prograde stage and T=910→730°C at the retrograde stage at P=3.5 GPa, which were preserved in high-pressure eclogitic inclusions (boudins, layers and lenses) of the lower part of the complex as a result of tectonic mélange.

The prograde and retrograde PT trends constructed from the phase compositions of the Grt-Cpx-Pl-Qz paragenesis form conjugated pairs characterizing the modes of individual stages (cycles) of the development of the complex (Table 1).

Figure 1 shows one of the numerous examples (Fedkin, 2020) of the inversion zoning of a garnet from an eclogitic boudin at the Antingan site. The composition of the garnet in equilibrium with Cpx, Pl, and Qz marks a successive transition from the PT conditions of tectonic mélange to the stage of coherent development of the rock of the host complex. Inclusions of residual and newly formed minerals (Cpx, Pl, Qz) in a zoned garnet grain allow us to trace its progressive growth and estimate the equilibrium pressure (P=1.35 GPa) at the initial stage of rock formation (**Fig. 1a**). Then the zoning of the garnet reverses, fixing a decrease in temperature: 617→518 °C in the process of coherent development of the host matrix (**Fig. 1c**). On regressive steel, garnet grains are gradually surrounded by Qz-Ms-Chl clusters, fracturing and fragmentation of garnet inclusions increase, traces of their rotation and movement in the mass of the host rock are noticeable.

Similar thermobaric processes are clearly recorded at each stage of development of the complex, while the petrochemical composition of high-pressure rocks (tholeiitic basalts) remains virtually unchanged (Volkova, et al., 2004; Leech and Ernst, 2000; Schulte and Blümel, 1999). Metasomatism at this stage is difficult due to the pulsating nature of metamorphism and the high buoyancy of the submerged plate. In the lower high-pressure part of the complex, the first signs of metasomatic changes appear at later stages of metamorphism in the form of muscovitization zones, veinlet accumulations of zoned garnets, and chlorite rims around the garnet. Textures of atoll and openwork garnet appear in garnet grains, confirming the presence of liquid under HP conditions (Beane and Sorensen, 2007). Only at the third stage, low-temperature phases Zo, Gln, Chl appear in eclogitic associations as a result of petrochemical processes (Valizer, 2011).

¹ Mineral symbols according to Whitney and Evans, 2010

Table 1. Generalized PT trends of prograde-retrograde stages (cycles) of development of the Maksyutov eclogite-glaucophane schist complex (Fedkin, 2020).

No.	Prograde trends	Retrograde trends	Age, Ma*
1.	T=800→900 °C, P=3,5 GPa	T=910→730 °C, P=3,5 GPa	515-533 [1, 3] 385 [2]
2.	T=500→790 °C, P=2,5→3,0 GPa	T=740→610 °C, P=2,5→1,4 GPa	360 [1, 2] 360-380 [3]
3.	T=460→680 °C, P=1,1→1,5 GPa	T=690→430 °C, P=1,3→1,0 GPa	335 [2]
4.	T=310→515 °C, P=0,9→1,2 GPa	T=545→310 °C, P=1,0→0,6 GPa	310-315 [2]

*) Age definitions are given according to: [1] - Valizer et al. 2013; [2] - Beane & Leech, 2007; [3] - Dobretsov et al., 1996.

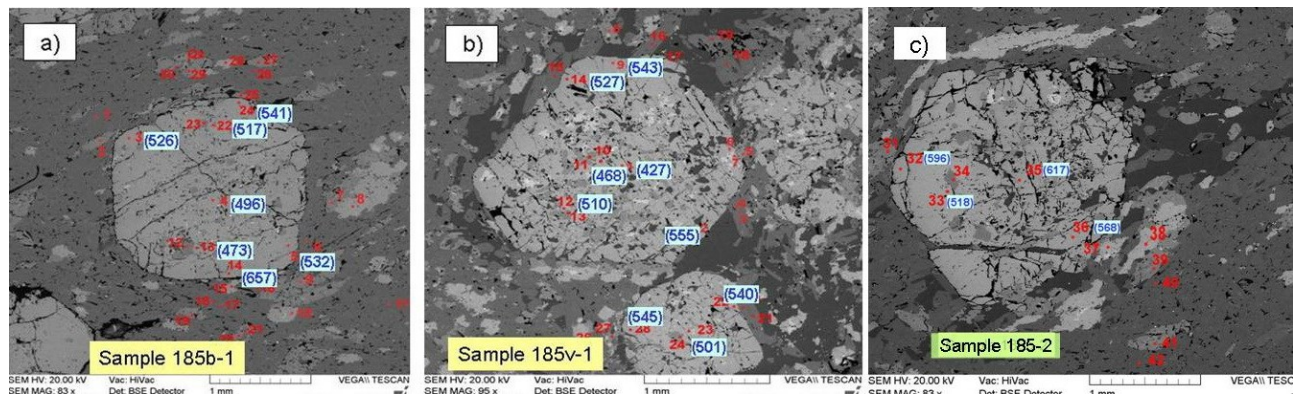


Fig. 1. Sequential prograde-retrograde development of the eclogitic boudina of the Antingan site during its inclusion in the coherent process of retrograde metamorphism: (a) prograde stage 473-657°C, (b) intermediate stage 427-555°C, (c) retrograde stage at coherent level of development of the complex 617-518 °C

In the upper (ophiolite) plate of the complex, in metasomatized basalts included in the antigorite serpentinite-matrix melange (Beane and Liou, 2005), Ca-Mg metasomatism results in the formation of rodingites and carbonate mineral associations, serpentinization of the surrounding peridotite, and crystallization of large crystals of lawsonite, which was subsequently replaced by muscovite, clinozoisite, and garnet. These signs show an increased level of pressure and the belonging of the upper rock member to the ophiolite-like facies series. Changes in the bulk composition of the rocks of the complex in terms of the main rock-forming components are not so noticeable due to the fact that most geochemical works usually focus on rare, trace and rare earth elements to study the geochemistry and the source of the protolith.

More distinct signs of metasomatic changes in the bulk composition of rocks appear at the end of tectonic melange processes at the coherent stage of terrane development. In the main part of the complex, in a series of rocks from unaltered eclogites to retrograde coarse-grained mica-bearing eclogites, a noticeable decrease in the content of Ca, Ti, Na and an increase in K is recorded (Beane and Sorensen, 2007). In the potassium metasomatized metabasalts of the upper part of the complex, an increase in the content of potassium is accompanied by an increase in the content of barium. The processes of further muscovitization of rocks of the complex and mass

formation of muscovite pseudomorphs after lawsonite are associated with potassium metasomatism (Schulte and Sindern, 2002; Beane and Liou, 2005). The decrease in sodium activity shows that the development of glaucophane rocks of the complex is not associated with the addition of sodium, but occurs due to the redistribution of Ca and Na between other phases.

At the final (fourth) stage of development of the complex, the coherent processes of the thermobaric and petrochemical plans proceed in opposite directions: along the line of retrograde metamorphism and an increase in the activity of metasomatic processes. This is expressed in a sharp decrease in the parameters of Grt-Cpx equilibria under the action of fluid flows, which increase the reactivity of the components dissolved in the fluid and reduce the effect of intense RT parameters of metamorphism due to the natural cooling of the ascending complex.

Findings and Conclusions

1. The initial competition of two opposite petrophysical processes of different levels - the tectonic melange of high-pressure eclogite inclusions and their subsequent joint coherent development with the enclosing gneissic matrix lead to the formation of contrasting series of rocks at an early stage of the formation of the complex and to their preservation until the final stages of metamorphism;

2. The combination of coherent processes of a

metamorphic (thermobaric) plan and a metasomatic (petrochemical) direction in different parts of the complex is realized in different ways. In the mafic member of the complex, the chemical composition of the original rocks remains almost unchanged. Signs of metasomatism are manifested only in the form of morphological changes in garnet or its replacement with zoisite or glaucophane. More noticeable processes of metasomatism are visible in the upper ophiolite part of the complex: the formation of lawsonite metasomatized basalts, rodingites, serpentinite melange, carbonate-bearing, actinolite and chlorite rocks. The reason for this may be the spatial disunity or temporal gap in the origin of these members.

3. The petrochemical processes of the mafic and ophiolite parts of the complexes differ significantly in the set of mobile elements: more basic (Mg, Fe, Ti, Ca) for eclogitic rocks, and easily mobile (Ca, K, Na, Al, Si) for ophiolite-like formations.

4. The final stage of the evolution of the complex is associated with a wave of acid leaching, which causes the processes of intense K–Ba muscovitization of the rocks of the entire complex.

5. The visible process of active glaucophanization of the rocks of the complexes is not associated with a significant addition of sodium, but is caused by the redistribution of Ca and Na among other minerals.

The work was carried out within the framework of the State Assignment FMUF-2022-0004, reg. No. 1021051302305-5-1.5.2 and the Fulbright Program of the Institute of International Education, grants 2011 and 2015.

The author thanks the director of the Limens State Reserve P.M. Valizer for help in field work, for creative discussion and useful discussion of the results.

References

- Beane R.J., and Liou J.G. Metasomatism in Serpentinite Mélange Rocks from the High-Pressure Maksyutov Complex, Southern Ural Mountains, Russia // International Geology Review. 2005. V. 47. P. 24–40.
- Beane, R., and Sorensen, S.S. Protolith signatures and element mobility of the Maksyutov subducted slab, Southern Ural Mountains, Russia: Inter. Geol. Review. 2007. V. 49. P. 52–72.
- Beane, R.J., Leech, M.L. The Maksyutov Complex: The first UHP terrane 40 years later. // Convergent Margin Terranes and Associated Regions // Geol. Soc. Am. Spec. Paper. 2007. V. 419. P. 153–169.
- Chesnokov and Popov, 1965 Increase in the volume of quartz grains in eclogites of the Southern Urals. // Dokl. AN SSSR 1965. V. 162. No. 4. Pp. 909–910. (In Russian)
- Dobretsov N.L., Sobolev N.V. 1977. Glaucophane-schist belts. // In the book. Metamorphic complexes of Asia. N: Science, pp.283–288. (In Russian)
- Dobretsov, N.L., Shatsky, V.S., Coleman, R.G., Lennykh, V.I., Valizer, P.M., Liou, J.G., Zhang, R., and Beane, R.J. Tectonic setting of ultrahigh-pressure metamorphic rocks in the Maksyutov Complex, Ural Mountains, Russia. // Intern. Geology Review. 1996. V. 38. P. 136–160.
- Fedkin V.V. Four episodes of thermal evolution of eclogites of the Maksyutov Complex (Southern Urals). // Geology and Geophysics, 2020. v.61. pp.666–684, DOI:10.15372/GiG2019182 (In Russian)
- Fedkin V.V. Mineralogical geothermobarometry in developing metamorphic systems. // On Sat. "Experimental mineralogy: some results at the turn of the century". 2004. M. Science, vol. 2, pp. 172–187. (In Russian)
- Fedkin, V.V., et al., 2021 Petrotectonic origin of mafic eclogites from the Maksyutov subduction complex, south Ural Mountains, Russia. // Geological Society of America Special Paper. 2021. V. 552, P. 177–195,
- Leech, M. L., and Ernst, W. G. Petrotectonic evolution of the high- to ultrahigh-pressure Maksyutov Complex, Karayanova area, south Ural Mountains, Russia: structural and oxygen isotopic constraints. // Lithos, 2000. V. 52. P. 235–252.
- Lennykh V.I., et al., Petrotectonic evolution of the Maksyutov Complex, Southern Urals, Russia: implications for ultrahigh-pressure metamorphism // Int. Geol. Rev., 1995, v. 37, p. 584—600.
- Schulte, B., and Sintern, S. K-rich fluid metasomatism at high-pressure metamorphic conditions: Lawsonite decomposition in rodingitized ultramafite of the Maksyutov Complex, southern Urals (Russia): Journal of Metamorphic Geology. 2002. V. 20. P. 529–541. doi: 10.1046/j.1525-1314.2002.00387.x.
- Schulte, B., and Sintern, S. K-rich fluid metasomatism at high-pressure metamorphic conditions: Lawsonite decomposition in rodingitized ultramafite of the Maksyutov Complex, southern Urals (Russia): Journal of Metamorphic Geology. 2002. V. 20. P. 529–541. doi: 10.1046/j.1525-1314.2002.00387.x.
- Sobolev N.S., Shatsky V.S. Problems of the genesis of eclogites of metamorphic complexes. // Geology and geophysics. 1986. No. 9. (In Russian)
- Valizer P.M. 2011 Garnet from eclogites of high-pressure complexes of the Urals. // Lithosphere. 2011. No. 5, p. 53–69 (In Russian)
- Valizer P.M. et al., “Jadeite-grossular eclogite of the Maksyutov Complex, Southern Urals,” Lithosphere. 2013. V. 4. S. 50–61. (In Russian)
- Volkova, N.L., et al., Geochemical signatures for eclogite protolith from the Maksyutov Complex, South Urals: Journal of Asian Earth Sciences. 2004. V. 23. P. 745–759.
- Whitney, D.L., Evans, B.W. Abbreviations for names of rockforming minerals. Am. Mineral. 2010. V. 95. P. 185–187.

Fedkin V.V.¹, Kotova L.S.^{1,2} Combined processes of eclogite-glaucophane schist formation: II Atbashi, Southern Tien Shan
UDC 549.6+552.16:552.48

¹D.S. Korzhinskii Institute of Experimental Mineralogy Russian Academy of Sciences vfedkin@iem.ac.ru; ²M.M. Adyshev Institute of Geology National Academy of Sciences of Kyrgyz Republic fedkin@chgnet.ru

Abstract. The paper series titled "Combined processes of eclogite-glaucophane schist formation" describes interconnected processes of metamorphic and metasomatic evolutions of the two crustal mafic eclogite complexes. Petrologic and petrochemical data on relatively deep Maksyutov (Southern Urals) rocks were discussed in the first part. This paper presents the results of study of the Atbashi complex formed under moderate pressure. Progressive thermobaric processes yield PT parameters of formation of the contrasting rock series - high-pressure eclogite boudins, blocks, interlayers and lenses within the low metamorphism gneiss and schist matrix. The regressive metamorphic stage is combined with metasomatic processes resulting in the change of bulk chemical composition, causing mineral reactions, dissolution and redeposition of mineral components. Coherent combination of these processes results in the complete formation of eclogite-glaucophane schist complexes.

Keywords: High-pressure metamorphism, thermobaric processes, petrochemical changes, Maksyutov complex, Atbashi eclogite-glaucophane schist complex, tectonic mélange, coherent processes, metamorphic PT evolution paths.

In Fedkin (2023), a theory of coherent formation of crustal mafic eclogites was applied to a relatively deep Maksyutov complex. In this paper, the same mechanism is considered for formation of the Atbashi complex (Southern Tien Shan) under relatively moderate pressure. Both complexes belong to the same Ural-Mongolian fold belt, are similar by their origins (temperature and age formation interval, petrologic types, etc.) but differ by their formation conditions and type of metamorphic and metasomatic processes. Evolution of the Atbashi eclogite-glaucophane schist complex was studied using the detailed petrographic analysis of mineral relationships, bulk chemical composition of the high pressure and the host rocks (Kotova, 1989), metamorphic evolution (Dobretsov, 1974; Dobretsov and Sobolev, 1977; Fedkin, 2004), which allowed to reveal the connection of the coherent metamorphic and metasomatic processes during the complex formation.

Petrographic analysis of mineral relationships in the high pressure and the host rocks revealed a sequence of transformations of initial eclogites and pyroxenites into low temperature schists, quartzites and muscovite quartzites schists (Fig. 1). The two independent ways of such transformations resulting

in formation of spatially separated low temperature groups of rocks of mafic and ophiolite composition (Fig. 1, left and right sides, resp.) from the high pressure boudins and blocks intruded during the process of tectonic mélange (Fig. 1, center) are determined. Petrographic variety of the Atbashi complex reflects both thermobaric (metamorphic) processes and petrochemical (metasomatic) alterations due to a changing fluid regime at different stages of the terrain formation.

Thermobaric evolution of the Atbashi rocks was studied by detailed microprobe analysis of mineral composition and zoning in the key Grt²-Cpx-Pl-Qz rock forming mineral assemblage - the major information source for high-pressure rock formation conditions. High-pressure eclogite boudins, interlayers and lenses preserved in their host gneiss-schist complex as a result of tectonic mélange at its early stage record the peak metamorphism parameters: P up to 11-13 kbar and T = 350-650 °C (Dobretsov, 1974; Dobretsov and Sobolev, 1977; Fedkin, 2004). The parent glaucophane schist complex was formed during the regressive stage of metamorphism along with the formation of the high-pressure eclogite bodies and blocks at P=2-7 kbar and T=300-600 °C.

The progressive garnet zoning ($X_{Prp}=0.24-0.56$) and the omphacite-rich pyroxene ($X_{Jd}=0.4-0.6$) in the core of large eclogite boudins and individual isolated bodies yield a positive PT trend of their formation during the stage of tectonic mélange (Fedkin, 2004). Near the contact with the host rocks, the Grt±Cpx+Gln and Grt±Cpx+Zo assemblages appear in eclogites and pyroxenites and then become transformed into Gln-Ms-Chl and Cb-Pl-Qz schists. The prograde PT paths shift towards the lower pressure field. At P=5-7 kbar, the Grt-Cpx equilibria record a clockwise turnaround followed by the coherent stage of the complex formation (Fig. 2).

The progressive zoning of Fe-Mg minerals reverses. The peak PT parameters computed based on Grt-Cpx-Pl-Qz equilibrium do not exceed P=5-6 kbar and T=550-600 °C. Secondary pyroxene with a minimal jadeite mole fraction ($X_{Jd}=0.03-0.08$) forms in the parent schists. The pyroxene of the latter composition in equilibrium with Grt, Pl and Qz yields PT values significantly different from HP conditions for eclogite formation. The stability temperatures for the "secondary" Grt-Cpx assemblages falls to T=300-400 °C at P=1.5-2.3 kbar.

² Mineral symbols according to Whitney and Evans, 2010

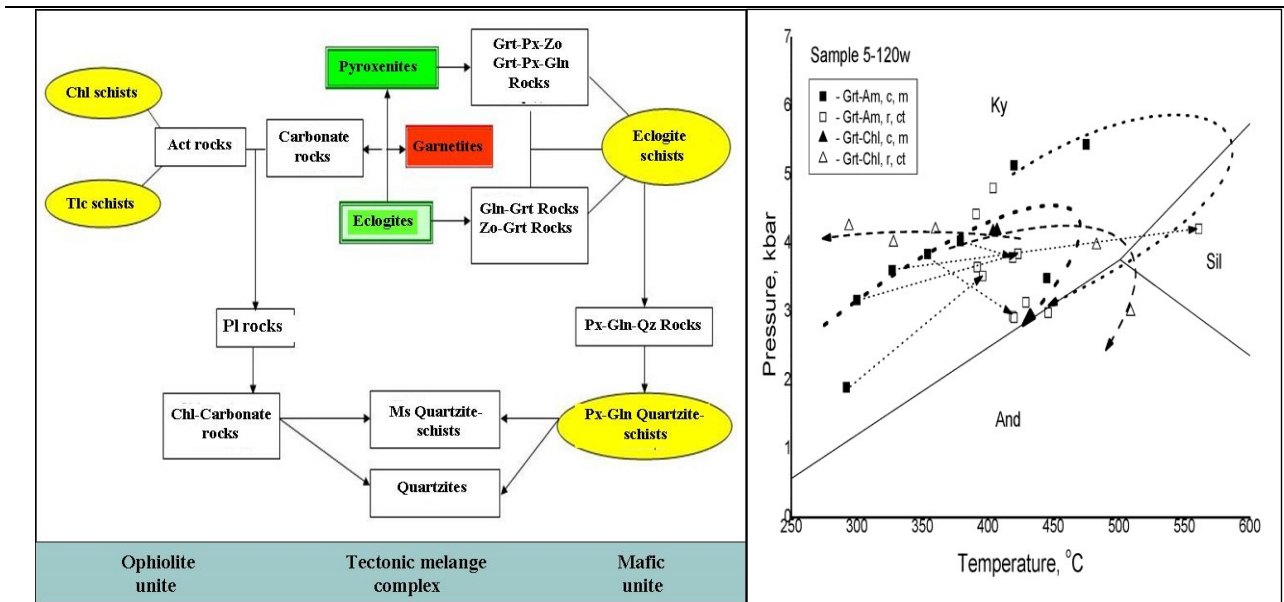


Fig. 1. The eclogite-glaucophane schist rock transformation in Atbashi Ridge (Kotova, 1989). Assignment of the individual rock types to the major lithological parts of the complex is shown.

Fig. 2. Thermobaric conditions for the Atbashi complex formation. The PT trend turnaround shows the transition from the tectonic mélangé stage to the coherent evolution (Fedkin, 2004).

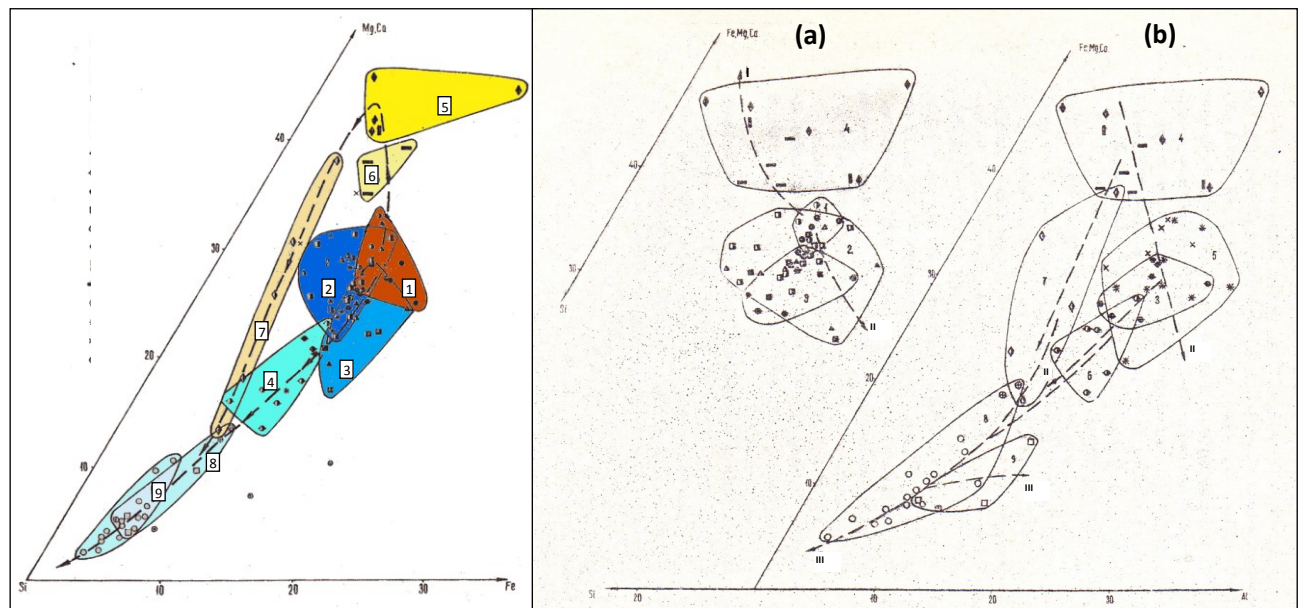


Fig. 3. The Si-Mg, Ca-Fe diagram for the Atbashi rock compositions. The contoured fields are for: 1 - eclogites and pyroxenites; 2 - Grt-Px-Gln and Grt-Px-Zo rocks; 3 - Gln-Grt and Zo-Grt rocks; 4 - Cpx-Gln-Qz rocks; 5 - Chl-Cc and Act rocks; 6 - Tlc schists; 7 - Chl-Cc-Qz rocks; 8 - quartzite schists; 9 - quartzites (Kotova, 1989).

Fig. 4. The Si-Fe, Mg,Ca-Al diagram. Cyrillic numbers - stages of rock transformation: (a) stages I and II and (b) stages II and III. The contoured fields are for: 1 - eclogites and pyroxenites; 2 - Gln and Zo rocks; 3 - eclogite schists; 4 - Chl-Cb, Act and Tlc rocks; 5 - Ab rocks; 6 - Px-Gln-Qz rocks; 7 - Chl-Cb-Qz rocks; 8 - Px-Gln quartzite schists; 9 - Mu quartzite schists.

Thermobaric evolution of the high-pressure mafic rocks (eclogites and pyroxenites) transported by tectonic mélangé was accompanied by the change in their bulk composition. At the first stage, alkalis, mostly Ca, and minor quantities of Fe, Mg, Na were removed from eclogites and pyroxenites replaced by Grt \pm -Cpx-Gln and Grt \pm -Cpx-Zo rocks (Fig. 3).

Removal of Ca and Fe causes a replacement of pyroxene by either glaucophane or zoisite, depending on the proportions of the removed components. Release of Fe and Mg results in the formation of secondary Fe-Mg minerals. Ophiolite-like assemblages containing carbonates, Srp, Tlc, Act, Chl and Pl sometimes occur among the metabasite

rocks. Such joint occurrences of the mafic and ophiolite rocks are due to various metasomatic processes, similar to the Tien Shan “C3 China” metaophiolite belt adjacent to the Atbashi complex from the Southern (Lú, Bucher, 2018).

The second stage of petrochemical changes occurs during transition from the stage of tectonic mélange to the coherent stage, at pressure falls to 5-7 kbar. The initial rock composition changes as a result of metasomatism in two ways. Calcium content falls from 30-35 wt. % to 20 wt. % in mafic rocks, but increases up to 40-50% in the ophiolite-like assemblages (Fig. 4, trends I and II). The Ab, Chl, Tlc bearing rocks form due to removal of Na and Al; Ep and Chl replace Zo and Grt. New fields of Tlc schists, Chl-Cc and Act containing rocks, and also the fields of Cpx-Gln-Qz and transitional Chl-Cc-Qz rocks form, as shown in Si-Mg, Ca-Fe diagram (Fig. 4). Intensive eclogites and pyroxenites carbonatization provides evidence of high carbon dioxide and Ca activities at this stage. Aluminum remains inert and is concentrated in muscovite and garnet.

The third stage is allochemical changes in the rocks by addition of silica and potassium resulting in more intensive silicification and muscovitization (Fig. 4b, trend III). This stage is characterized by low metamorphism parameters. Leaching of eclogites and pyroxenites removes Ca, Fe, Mg and then Na and Al. High carbon dioxide activity provokes addition of silica and potassium. The glaucophane rock formation occurs without addition of sodium due to sodium and calcium redistribution between the carbonate phases and plagioclase (Dobretsov, 1974; Kotova, 1989). Muscovitization and intensive silicification of rocks with muscovite quartz schist and quartzite formation then occur by introduction of silica and potassium.

The reasons for joint occurrence of different types of metasomatic formations after the same source rocks can be a spatial separation of individual parts of the complex with their subsequent unification, or a temporal break and change in the fluid regime during metasomatism. The former is supported by petrographical observations, the latter - by occurrence of secondary carbonate lenses in mafic rocks and garnet and pyroxene recrystallization in the parent rocks with formation of “secondary eclogites” and carbonate bearing rocks containing Chl, Act, Tlc, Ab and Srp. Both mechanisms may be due to the influence of the nearby “NW China” metaophiolite belt in the southern part of the Atbashi terrane (Lú, Bucher, 2018). At the final stage of the complex formation, both processes are overlapped by the powerful acid leaching and alkali metasomatism event that erases the discrepancy between them and leads to widespread muscovitization and

silicification.

Conclusions

1. The Atbashi high-pressure eclogite rocks and glaucophane schists (eclogite bodies and boudins) formed at the early stage of the complex formation during the process of tectonic mélange. The parent gneiss-schists including Grt-Cpx rocks, Cpx-Gln, mica and chlorite schists, quartzites and quartzites schists formed at a later stage of regressive metamorphism during their joint coherent evolution as a single metamorphic cycle.

2. The petrographic variety of the Atbashi rocks is explained by the petrochemical analysis and is a result of subsequent rock transformation rather than the source rock heterogeneity.

3. Combination of metasomatic processes of mafic and ophiolite character is due to either their spatial separation, or temporal break, with the influence of the “NW China” ophiolite belt adjacent to the Atbashi complex as its structural continuation.

4. The Atbashi glaucophane rocks formed by removal of Ca and Na from eclogites without an extra addition of sodium.

The work was conducted within the frame of the FMUF-2022-0004 government project, reg. no.1021051302305-5-1.5.2 and a Fulbright program of the Institute of International Education in 2011 and 2015.

Authors thank colleagues A.B. Bakirov and V.A. Kotov, IG NAN Kyrgyzstan, for help with the field trip organization and fruitful discussions of the obtained results.

References

1. Bakirov A.B. and others. Conditions for Tien Shan eclogite formation. // *Sov. Geology* 1985. No. 2 (In Russian).
2. Beane, R.J., Leech, M.L. The Maksyutov Complex: The first UHP terrane 40 years later. // *Convergent Margin Terranes and Associated Regions* // *Geol. Soc. Am. Spec. Paper.* 2007. V. 419. P. 153–169.
3. Dobretsov N.L. Glaucophane and eclogite-glaucophane schist complexes of the USSR. Novosibirsk: Nauka, 1974. 217p. (In Russian).
4. Dobretsov N.L., Sobolev N.V. Glaucophane schist belts. // In book: *Metamorphic complexes of Asia*. N: Nauka, 1977. S. 283-288 (In Russian).
5. Dobretsov, N.L., Shatsky, V.S., Coleman, R.G., Lennykh, V.I., Valizer, P.M., Liou, J.G. Zhang, R., and Beane, R.J. Tectonic setting of ultrahigh-pressure metamorphic rocks in the Maksyutov Complex, Ural Mountains, Russia. // *Intern. Geology Review.* 1996. V. 38. P. 136-160.
6. Fedkin V.V. Combined processes of eclogite-glaucophane schist formation: I. Maksyutov complex (Southern Urals). // In book: “WESEMPG-2023”; *Proceedings of the All-Russian annual seminar on*

- experimental mineralogy, petrology and geochemistry. M.: GEOKHI 2023. S. XX-XX.
7. Fedkin V.V. The four stages of thermal evolution of the Maksyutov eclogite complex (Southern Urals). // *Geology and Geophysics*, 2020. v. 61. pp. 666-684, DOI:10.15372/GiG201918.
 8. Fedkin V.V. Mineralogical geothermobarometry for evolving metamorphic systems. // In book: "Experimental mineralogy: Some of the results of the past century". M. Nauka, 2004. V. 2, S. 172-187 (In Russian).
 9. Kotova L.S. Petrochemical evolution of the Atbashi Ridge eclogite-glaucophane schist complex (Southern Tien Shan). // In book: *Geochemistry of Tien Shan igneous and metamorphic formations*. Frunze: Ilim. 1989. S. 110-127 (In Russian).
 10. Lennykh V.L., Valizer P.M. High-pressure metamorphic rocks of the Maksyutov complex (Southern Urals) // 4th International Eclogite Field Symposium: field guide book. Novosibirsk. UIGGM SB RAS. 1999. 64 P
 11. Lü Z., Bucher K. The coherent ultrahigh-pressure terrane of the Tianshan meta-ophiolite belt, NW China. // *Lithos*, 2018, V. 314-315. P. 260-273.
 12. Sobolev N.V., Shatsky V.S. Problems of the genesis of eclogites of metamorphic complexes. // *Geology and geophysics*. 1986. No. 9 (In Russian).
 13. Whitney, D.L., Evans, B.W. Abbreviations for names of rock forming minerals. *Am. Mineral.* 2010. V. 95. P. 185–187.

Gorbachev N.S., Kostyuk A.V., Nekrasov A.N., Gorbachev P.N., Sultanov D.M. Distribution of Co, Ni, Re, Os, Pt between Fe-metallic and Fe-sulphide melts in the Fe–FeS–C system at 4 GPa, 1400 °C: fractionation, chalcophilic and siderophilic properties *UDC 123.456*

Korzinskii Institute of Experimental Mineralogy RAS
gor@iem.ac.ru, nastya@iem.ac.ru

Abstract. In the Fe–FeS–C system at 4 GPa, 1400°C, the partition coefficients D (Mc/Ms) and distribution coefficients K_d (Mc/Ms) of Fe, Co, Ni, Re, Os, Pt between Fe-metallic (Mc) and Fe-sulfide (Ms) melts were obtained. D (Mc/Ms) served as indicators of the siderophilic and chalcophile properties of each of the elements, K_d (Mc/Ms) characterized their interelement ratios during fractionation. In the Fe–Os–Co–Re series with D (Mc/Ms) > 1, siderophilic properties predominate, which increase with increasing D (Mc/Ms): 1,2-1,5-1,6-12,6. In the series Ni–Pt–S with D (Mc/Ms) < 1, chalcophile properties predominate, which increase with decreasing D (Mc/Ms): 0,9-0,6-0,1. K_d (Mc/Ms) Re/Os (8,4), Pt/Os (0,4) indicate the fractionation of Re and Pt with respect to Os, the shift of Re/Os and Pt/Os ratios and related systems $^{187}\text{Re}/^{187}\text{Os}$ и $^{190}\text{Pt}/^{186}\text{Os}$ isotopes. Based on the model of Mc–Ms liquation during the formation of sulfide mineralization in the Norilsk region, in the Norilsk-type intrusions the ratio Re/Os < 3 is similar to the Ms component, and in the Nizhne-Norilsk-type intrusions it is similar to the Ms component, Re/Os > 10. Pt

/Os ratios in pyrrhotite ores are higher than in experimental Mc and Ms melts.

Keywords: liquation, metal, sulfide, experiment, distribution of element

Melting and phase relations in the basalt–FeS–Fe–C system are of interest in connection with problems of early magmatic ocean (MO) differentiation, phase and chemical composition of meteorites with formation of their metallic cores and silicate mantle, as well as magmatic iron-sulfide deposits. This interest is due to the fact that during contamination of the sulfide melt with carbon there is a stratification of the sulfide melt into Fe-metallic (Mc) and Fe-sulfide (Ms) melts, immiscible with silicate ones. The formation of MO (chondritic composition of protomatter) and magmatic sulfide mineralization of the Norilsk area (composition of the platform cover and basement) do not exclude the formation of Mc–Ms melts in these processes.

Mc and Ms melt immiscibility were first observed in basaltic glasses of effusive rocks on Is. Disko, Greenland (Pedersen, 1979), experimentally considered in works (Gorbachev and Osadchii, 1980; Gorbachev et al., 1980). A sensitive indicator of these processes is the distribution of Re, Os, Pt, Ni, Co between Mc, Ms and silicate (L) melts. Geochemically, these elements are characterized by dual properties: siderophile, in the processes of early MO differentiation with separation of Ms melt (core) from L melt (primitive mantle); chalcophile, in the processes of magmatic sulfide deposit formation with Ms–L liquation. In Mc–L equilibria these elements are effectively concentrated in Ms melt with partition coefficients D Mc/L reaching 3–6 orders of magnitude (Righter, 2011; Siebert et al., 2011; Mann et al., 2012; Brenann et al., 2016). In Ms–L equilibria, these same elements also have chalcophile properties with D Ms/L reaching also 3–6 orders of magnitude (Naldrett, 1989; Fleet et al., 1996; Kiseeva, Wood, 2013; Mungall, Brenan, 2014). It is of geochemical interest to find out which properties, siderophile or chalcophile, prevail in each of these elements.

The fractionation of Re, Os, Pt, Ni, Co during Mc–Ms stratification of sulfide melts affects the concentrations and inter-element ratios of these elements in Mc, Ms and L melts. The evaluation of this influence is of interest given that the $^{187}\text{Re}/^{187}\text{Os}$ and $^{190}\text{Pt}/^{186}\text{Os}$ isotope systems based on the β -decay of ^{187}Re to ^{187}Os and α -decay of ^{190}Pt to ^{186}Os are associated with Re/Os and Pt/Os ratios, which will shift when the Re/Os and Pt/Os ratios change due to fractionation between Mc and Ms melts.

To estimate the siderophile and chalcophile properties of Co, Ni, Re, Os, Pt and their inter-element ratios the results of experimental study of the

distribution of Co, Ni, Re, Os, Pt between Mc and Ms melts formed during Mc-Ms splitting of C-bearing sulfide melt in Fe-FeS-C system at 4 GPa, 1400°C were used (Gorbachev et al., 2022).

The experiment was carried out at IEM RAS on an anvil with a hole using the multi-ampere quenching technique (Gorbachev, 1990) at 4 GPa, 1400°C for a duration of 4 hours. Temperature was measured by Pt30Rh/Pt6Rh thermocouple, pressure at high temperatures was calibrated by quartz-coesite equilibrium. The accuracy of temperature and pressure determination is estimated to be $\pm 10^\circ\text{C}$ and ± 1 kbar (Litvin, 1990). A finely ground mixture of synthetic pyrrhotite $\text{Fe}_{0.94}\text{S}_{1.0}$ (70 wt.%), metallic Fe (23 wt.%) and technical carbon (7 wt.%) with the addition of metallic Os, Re, Pt was loaded into a graphite ampoule, then this ampoule was placed into a Pt ampoule which was hermetically sealed. After the experiment, the ampoule was opened and pressed

into polystyrene. The polished samples were studied and analysed on a microprobe at IEM RAS.

During the melting of the initial ore fraction, the low-melting fraction is represented by a sulfide melt that has undergone Mc-Ms separation, forming interlayers of massive sulfides during quenching, the matrix of which contains microinclusions of the quenching Fe-metal phase and inclusions of globules of the Fe-metal phase ranging in size from 5 to 20 μm (Fig. 1).

Table 1 shows the concentrations of Co, Ni, Re, Os, Pt and interelement ratios in the Mc and Ms phases, as well as the partition coefficients of each of the elements D Mc/Ms and the distribution coefficients of 2 elements between Mc and Ms melts, characterizing their chalcophile and siderophilic properties. The partition coefficients of each of the elements D (Mc/Ms) are shown in Fig. 2.

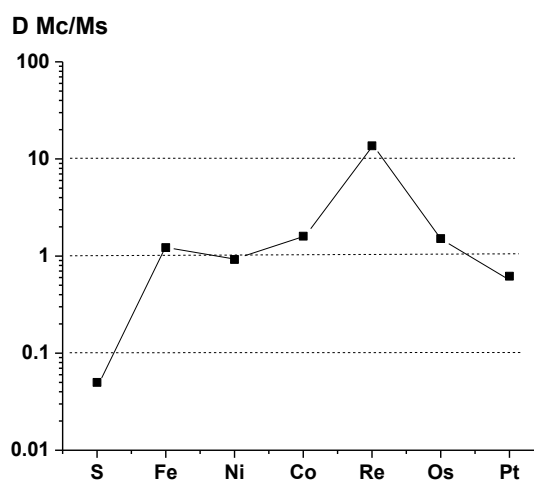
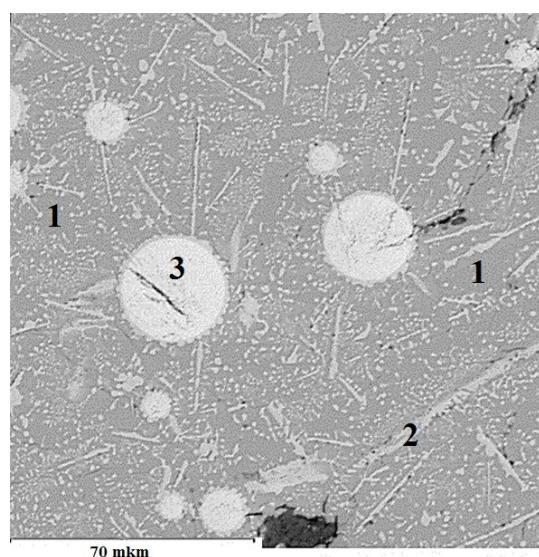


Fig. 1. BSE image of quenched sulfide melt: 1 – matrix, 2 – microinclusions of quenching Fe-metal phase, 3 – inclusions of globules of Fe-metal phase.

Fig. 2. Partition coefficients of ore elements between Mc and Ms melts.

Table 1. Concentrations of ore-forming elements in Mc and Ms phases, coefficients of partition and distribution of these elements between Mc and Ms melts.

Elements	C, wt.% (Mc)	C wt.% (Ms)	D Mc/Ms
S	1.45 \pm 0.49	26.68 \pm 0.56	0.05
Fe	88.18 \pm 1.69	72.18 \pm 0.80	1.22
Ni	0.37 \pm 0.15	0.40 \pm 0.12	0.92
Re	9.96 \pm 1.49	0.79 \pm 0.45	12.61
Os	0.54 \pm 0.16	0.36 \pm 0.06	1.50
Pt	0.39 \pm 0.22	0.63 \pm 0.10	0.62
Co	1.28 \pm 0.16	0.80 \pm 0.18	1.60
Ratios	Mc n=21	Ms n=16	Kd Mc/Ms
Re/Os	18.44	2.20	8.38
Pt/Os	0.72	1.75	0.41
Re/Pt	25.54	1.25	20.43
Ni/Co	0.29	0.50	0.58

Estimation of chalcophilic and siderophilic properties of Co, Ni, Re, Os, Pt, coefficients of separation of each of the elements D (Mc/Ms) between Mc and Ms melts.

The indicator of siderophilic and chalcophile properties - the relative affinity of an element for the Mc and Ms phases are the partition coefficients of each of the elements between Mc and Ms melts, expressed as the ratio of the weight concentrations (C) of a given element in the Mc melt to its concentration in the Ms melt: $D (Mc / Ms) = C(Mc)/C(Ms)$. In elements with $D (Mc/Ms) = 1$, siderophile and chalcophile properties are manifested in the same way. Elements with $D (Mc/Ms) > 1$ are dominated by siderophilic properties, while those with $D (Mc/Ms) < 1$ are dominated by chalcophile properties. The more the $D (Mc/Ms)$ values differ from 1, the stronger the siderophilic properties (at $D > 1$) or chalcophile properties (at $D < 1$).

As can be seen from the table 1 and Fig. 2 data, for Fe, Co, Re, Os, the partition coefficients $D (Mc/Ms) > 1$, therefore, for each of these elements, siderophilic properties prevail over chalcophilic ones. Siderophilic properties increase with increasing $D (Mc/Ms)$ 1.22-1.50-1.60-12.61 in the sequence $Fe < Os < Co < Re$. In this series, the strongest affinity for the Fe-metal phase (siderophilicity) is Re, with $D (Mc/Ms) = 12.61$. Other elements of the series - Fe, Os, Co are characterized by less contrasting differences in siderophilic and chalcophilic properties with low (< 2) $D (Mc/Ms)$ values.

In the series of elements S, Ni, Pt with $D (Mc/Ms) < 1$, chalcophilic properties predominate, which increase with decreasing $D (Mc/Ms)$ in the sequence $Ni < Pt < S$. An increase in chalcophilicity is characterized by separation factors $D (Mc/Ms)$, which decrease in the sequence: 0.92-0.62-0.05. Ni and Pt with low $D (Mc/Ms)$ values are characterized by less contrasting differences in siderophile and chalcophile properties. Significant $D (Mc/Ms)$ of sulfur indicate its solubility in Fe-metal melts.

Fractionation of Co, Ni, Re, Os, Pt at Mc and Ms liquation, distribution coefficients of 2 elements between Mc and Ms melts.

The indicator of interelement ratios of Re, Co, Ni, Os and Pt during fractionation as a result of Mc

and Ms liquation of sulfide melts are the distribution coefficients of 2 elements. For example, Re and Os between Mc and Ms melts characterize the exchange reactions of these elements during distribution between Mc and Ms melts: $Re(Ms)+Os(Mc) = Re(Mc)+Os(Ms)$, from the equilibrium constant of which, assuming ideality of the exchange reaction follows: $Kd_{ij} (Mc / Ms) = (C_i/C_j) Mc/(C_i/C_j) Ms = D_i (Mc) / D_j (Ms)$.

In the association of Re-Os and Re-Pt, high values of the distribution coefficient $Kd Mc/Ms Re/Os$ (8.38) and $Kd Mc/Ms Re/Pt$ (20.43) indicate effective fractionation of Re relative to Os and Pt due to redistribution Re into the Fe-metal phase. This effect will lead to underestimated Re/Os and $^{187}Re/^{187}Os$ ratios in the Ms melt and abnormally low Re/Pt ratios in the Ms melt.

In the association of Pt-Os and Ni-Co, based on the values of $Kd Mc/Ms Pt/Os = 0.41$ and $Kd Mc/Ms Ni/Co = 0.58$ at Mc-Ms liquation, one can expect underestimated ratios of Pt/Os and Ni-Co in Ms melt versus Ms melt. However, the relatively low values of $Kd Mc/Ms Pt/Os$ and Ni/Co (0.41 and 0.58) indicate not so significant variations in the Pt/Os, $^{190}Pt/^{186}Os$, and Ni/Co ratios during Mc and Ms separation.

Geological application. In the work (Gorbachev et al., 2021), the possibility of the participation of Mc and Ms liquation in the formation of sulfide mineralization during the trap magmatism of the Norilsk region was considered. The Re/Os and Pt/Os ratios in magmatic sulfides from the region's intrusions and in experimental Mc and Ms melts can serve as an indicator of such a process. Table 2 shows the Re/Os ratios in sulfides of the intrusive complexes of the Norilsk region.

Since Pt concentrations increase from pyrrhotite to chalcopyrite types of ores during crystallization differentiation of sulfide melt, while Os concentrations remain constant (Gorbachev, 2006), the Pt/Os ratios in sulfides were estimated using Pt and Os contents in the least differentiated, pyrrhotite ores (table 3).

Table 2. Re/Os ratios in sulfides of intrusive complexes of the Norilsk region and experiment.

Type of mineralization	Intrusions	Re/Os*
Norilsk type	Norilsk I	1,61
	Talnakhsky	0,98 (1,0-2,4)
	Kharaelakhsky	1.76 (1,6-8,8)
	M. Chernaya	0,65
	M. Zub	2,7 (1,9-3,5)

Type of mineralization	Intrusions	Re/Os*
	South Pyasina	1.60 (1,0-2,2)
	Vologochansky	2,25 (1,9-2,6)
Nizhne-Norilsk type	Nizhny Talnakhsy	17,65 (13,7-21,6)
	Nizhny Norilsk	11, 80 (6,5-17,1)
Experiment	Mc	18,44
	Ms	2,20

Note: * data (Adamskaya et al., 2017)

Table 3. Distribution of Pt and Os in pyrrhotite ores of intrusive complexes of the Norilsk region and experiment.

Intrusions		Pt, ppm	Os, ppm	Pt/Os
Norilsk I		30461 ± 25108 n=11	295 ± 275 n=11	103.3
Kharaelakhsky		2705 ± 1057 n=16	22,3 ± 16,3 n=12	121,3
Talnakhsy		2049 ± 2015 n=11	76,4 ± 46,0 n=11	26,8
Experiment	Mc	0.39 ± 0.22 n=21	0.54 ± 0.16 n=16	0.72
	Ms	0.63 ± 0.10 n=21	0.36 ± 0.06 n=16	1.75

The Pt/Os ratio in the sulfides of the Norilsk 1 and Kharaelakh intrusions is of the same order, 101.4 and 121.2, and the lower ones are in the sulfides of the Talnakh intrusion - 26.8.

Thus, based on the model of Mc-Ms liquation during the formation of sulfide mineralization in the Norilsk region, in the Norilsk-type intrusions the ratio Re/Os < 3 is similar to the Ms component, and in the Nizhne-Norilsk-type intrusions it is similar to the Ms component, Re/Os > 10. The Pt/Os ratios in pyrrhotite, the least differentiated ores of the deposits of the Talnakh ore cluster, are higher than in the experimental Mc and Ms melts.

This study is fulfilled under Research program № FMUF-2022-0001 of the Korzhinski Institute of Experimental Mineralogy, with the support of the Russian Science Foundation grant No. 21-17-00119.

References:

Adamskaya E.V., Badinova V.P., Belyatsky B.V. and others. Isotope geology of the Norilsk deposits. Ed. VSEGEI. Saint Petersburg. 2017

Brenan J. M., Bennett N. R., Zajacz Z. Experimental results on fractionation of the highly siderophile elements (HSE) at variable pressures and temperatures during planetary and magmatic differentiation // *Reviews in Mineralogy and Geochemistry*. 2016. V.81(1). 1-87.

Fleet, M. E., Crocket, J. H., Stone, W. E. Partitioning of platinum-group elements (Os, Ir, Ru, Pt, Pd) and gold between sulfide liquid and basalt melt // *Geochimica et Cosmochimica Acta*. 1996. V. 60. N.13. P. 2397-2412.

Gorbachev N.S. Fluid-magma interaction in sulfide-silicate systems // *International Geology Review*. 1990. V. 32. №. 8. P. 749-836

Gorbachev N.S. Mineralogical and geochemical zoning and genesis of massive sulfide ores at the Oktyabr'sky deposit. *Geology of Ore Deposits*, 2006, 48, 473-488.

Gorbachev N.S. Sources and formation conditions of sulfide-silicate magmas in the Noril'sk district. *Geology of Ore Deposits*, 2012, 54, 155-178.

Gorbachev N.S., Kostyuk A.V., Nekrasov A.N., Gorbachev P.N., Soultanov D.M. Melting and phase relations in the basalt-FeS-Fe-S system at P=4 GPa, T=1400°C: Re behavior at FeS-FeC liquation of a Fe-S-C melt // *Experiment in Geosciences*. 2022. V. 28, No. 1. P. 46-49

Gorbachev N.S., Osadchii E.G., Baryshnikova G.V. Immiscibility in Ore-Silicate Melts as a Factor in the Early Differentiation of Meteorites and Planets // *Lunar and Planetary Science Conference*. 1980. V. 11. P. 348-350.

Gorbachev N.S., Osadchii E.G. Immiscibility in melts as a factor in the early differentiation of meteorites and planets // *Reports of the Academy of Sciences of the USSR*. 1980. V. 255. No. 3. S. 693-697.

Gorbachev N.S., Shapovalov Yu.B., Kostyuk A.V., Gorbachev P. N., Nekrasov A.N., Sultanov D.M. Phase relations in the Fe-S-C system at P=0.5 GPa, T=1100-1250°C: Fe-S-C liquation and its role in the formation of magmatic sulfide deposits // *Doklady Earth Science*, 2021, Vol. 497(1), p. 206-210

Kiseeva E.S. and Wood B.J. A simple model for chalcophile element partitioning between sulphide and silicate liquids with geochemical applications // *Earth Planet. Sci. Lett*. 2013. 383, 68-81.

Litvin Yu.A. Physico-chemical studies of the melting of the deep matter of the Earth. M.: Science. 1991. 312 C.

- Mann U., Frost D. J., Rubie D. C., Becker H. and Audertat A. Partitioning of Ru, Rh, Pd, Re, Ir and Pt between liquid metal and silicate at high pressures and high temperatures—Implications for the origin of highly siderophile element concentrations in the Earth's mantle // *Geochim. Cosmochim. Acta*. 2012. 84, 593–613.
- Mungall J. E. and Brenan J. M. Partitioning of platinum-group elements and Au between sulphide liquid and basalt and the origins of mantle-crust fractionation of the chalcophile elements // *Geochim. Cosmochim. Acta*. 2014. 125, 265–269.
- Naldrett A.J. *Magmatic Sulfide Deposits*. Oxford Monographs on Geology and Geophysics. No 14. 1989.
- Pedersen A. K. Basaltic glass with high-temperature equilibrated immiscible sulphide bodies with native iron from Disko, central West Greenland // *Contributions to Mineralogy and Petrology*. 1979. V. 69. No. 4. P. 397–407.
- Righter, K. Prediction of metal–silicate partition coefficients for siderophile elements: An update and assessment of PT conditions for metal–silicate equilibrium during accretion of the Earth. *Earth and Planetary Science Letters*, 2011, 304(1-2), 158-167.
- Siebert J., Corgne A. and Ryerson F. J. Systematics of metal–silicate partitioning for many siderophile elements applied to Earth's core formation. *Geochim. Cosmochim. Acta*, 2011, 75, 1451–1489.

Iskrina A.V.^{1,2}, Bobrov A.V.^{1,2,3}, Spivak A.V.², Zakharchenko E.S.², Khasanov S.S.⁴, Kuzmin A.V.⁴ Experimental *in situ* investigation of postspinel phases in the Mg-Al-Cr-O system up to 30 GPa UDC 549.02

¹Lomonosov Moscow State University, Moscow, ²D.S. Korzhinskii Institute of Experimental Mineralogy RAS, Chernogolovka, ³Vernadsky Institute of Geochemistry and Analytical Chemistry RAS, Moscow, ⁴Institute of Solid State Physics RAS, Chernogolovka (iskrina.av888@gmail.com)

Abstract. In the subduction zones, the mantle depths are enriched by crustal matter. Basalt, in comparison with pyrolite, contains higher concentrations of SiO₂, Al₂O₃, CaO, FeO, Na₂O, K₂O. It is assumed that the so-called postspinel phases (Akaogi et al., 1999) with structures of calcium ferrite, calcium titanate and marokite are concentrators of crustal elements in the transition zone and the lower mantle. In this work, an *in situ* study of the Mg-Al-Cr-O system was carried out. The phases of Mg₂(Al,Cr)₂O₅ and Mg(Cr,Al)₂O₄ composition were synthesized. The Mg₂(Al,Cr)₂O₅ phase has a modified ludwigite (*Pbam*) structure, and the Mg(Cr,Al)₂O₄ phase has a calcium titanate structure and crystallizes in the *Cmcm* space group. It was studied up to 30 GPa in a diamond anvil cells. As a result, it was found that at 12-16 GPa the color of the crystal changes from green to red, which persists with a further increase in pressure. This change is not stable, as the pressure decreases, the crystal turns green again. The phases described above are undoubtedly stable in mantle conditions and can be

considered as host-phases for crustal elements in the Earth's mantle.

Keywords: *post-spinel phases, transition zone, lower mantle, structure, in situ investigation, structure, IR-spectroscopy*

Spinel is a widespread mineral found in various geological environments. In the study (Ringwood, 1975), it was suggested that phases with calcium ferrite CaFe₂O₄ (CF), calcium titanate CaTi₂O₄ (CT) and marokite-type structure can be considered as postspinel phases in the conditions of the Earth's mantle (Decker, Kasper, 1957, Rogge et al., 1998, Giesber et al., 2001). The structure of the post-spinel phases is formed by edge and corner octahedra with channels parallel to the *b* axis (CF structure) and the *a* axis (CT structure), respectively. These two structures contain AO₈ octahedra and NBO₆ octahedra. There are two types of octahedral BO₆ positions in the CF structure and one type of octahedral BO₆ position in the CT structure. Among the post-spinel structures, there are structures with centered *Cmcm* (*Bbmm*) and primitive *Pnma* (*Pmcn*), *Pbcm* (*Pmab*) cells.

In the subduction zones, the mantle depths are enriched by crustal matter. Basalt, in comparison with pyrolite, contains higher concentrations of SiO₂, Al₂O₃, CaO, FeO, Na₂O, K₂O. It is assumed that the so-called post-spinel phases (Akaogi et al., 1999) with structures of calcium ferrite, calcium titanate and marokite are concentrators of crustal elements in the transition zone and the lower mantle. In this work, an *in situ* study of the Mg-Al-Cr-O system was carried out.

The experiments were carried out using a 1200-t multi-anvil Sumitomo press at the Bayerisches Geoinstitut (Bayreuth, Germany). The starting powders were homogenized in the agate mortar and then annealed in platinum crucibles for 24 hours at 1000°C. The ready starting mixture was placed into a capsule made of a 0.25 mm platinum foil. Experiments on multi-anvil press were carried out using standard 7/3 assemblages. Experiments on the synthesis of phases in the Mg-Al-Cr-O system at pressures of 22 and 24 GPa and a temperature of 1600°C with an exposure time from 1 to 5 hours. The phase composition was determined using a scanning electron microscope CamScanM2300 (VEGA TS 5130MM) with the Link INCA spectral analyzer in the IEM RAS. The accelerating voltage was 20 kV. The beam current was ~10nA. The average of compositions of the studied phases was determined by 8 analyses.

The structure of newly formed phases was determined by single-crystal X-ray diffraction using a Bruker SMART APEX CCD diffractometer with Rigaku rotating anode (Rotor Flex FR-D, Mo-K α

radiation) and Osmic focusing X-ray optics at the Bayerisches Geoinstitut, Germany and Rigaku Oxford Diffraction "Gemini R" CCD diffractometer with graphite monochromated MoK α radiation ($\lambda=0.71073$ Å) at the Institute of Solid State Physics RAS.

Raman spectra of experimental samples were obtained using an Acton SpectraPro-2500i spectrograph with a CCD Pixis2K cooling detector up to -70C and an Olympus microscope with a 532 nm monomeric laser at Institute of Experimental Mineralogy RAS.

In experiments at pressures of 22 and 24 GPa, the Mg₂(Al,Cr)₂O₅ and Mg(Cr,Al)₂O₄ phases were synthesized. They are green crystals ranging in size from 30 to 60 μ m. Single crystals were selected for further research.

The Mg₂(Al,Cr)₂O₅ phase has a modified ludwigite (*mLd*) structure (*Pbam* space group), which was also observed for Mg₂Al₂O₅ and Fe₂Cr₂O₅ compounds (Enomoto et al., 2009). It is possible that this structure is "intermediate", excluding the possibility of a direct transition from a calcium ferrite to a calcium titanate structure in a certain pressure range. However, this assumption requires further clarification.

The Mg(Cr,Al)₂O₄ phase has a calcium titanate structure and crystallizes in the *Cmcm* space group. It was studied up to 30 GPa in a diamond anvil cell. As a result, it was found that when the crystal reaches 12-16 GPa, the color of the crystal changes from green to red, which persists even with a further increase in pressure. This change is not stable, and when the pressure decreases, the crystal turns green again. This effect is associated with the contribution of the trigonal component to the octahedral coordination of (Cr,Al)O₆, as a result of which the parameter $-3/2K$ changes. Below a pressure of 6 GPa, compression is mostly isotropic, but above this value, the trigonal distortion increases rapidly with pressure (Sugano et al., 1958).

Based on the results of this study, it can be concluded that in the Mg-Al-Cr-O system, the presence of a phase with the structure CT and a phase with the *mLd* structure is observed. The above-described phases are undoubtedly stable under mantle conditions, can be considered as postspinel phases and as a concentrators of aluminum and other elements in the deep layers of the Earth.

This study was supported by the Russian Science Foundation (project №21-17-00147), Russian Foundation for Basic Research, project №20-35-90095. This study carried out within the scientific plan of the Laboratory of deep geospheres of the Lomonosov Moscow state University and within the Research Program of the D.S. Korzhinskii Institute

of Experimental Mineralogy Russian Academy of Sciences (FMUF-2022-0001).

References

- Akaogi M., Hamada Y., Suzuki T., Kobayashi M. and Okada M. (1999) High pressure transitions in the system MgAl₂O₄-CaAl₂O₄: A new hexagonal aluminous phase with implication for the lower mantle. *Phys. Earth Planet. Inter.* **115**, 67–77.
- Decker B. F. and Kasper J. S. (1957) The structure of calcium ferrite. *Acta Crystallogr.* **10**, 332–337.
- Giesber H. G., Pennington W. T. and Kolis J. W. (2001) Redetermination of CaMn₂O₄. *Acta Crystallogr. Sect. C Cryst. Struct. Commun.* **57**, 329–330.
4. Reid A. F. and Ringwood A. E. (1969) Newly observed high pressure transformations in Mn₃O₄, CaAl₂O₄, and ZrSiO₄. *Earth Planet. Sci. Lett.* **6**, 205–208.
5. Rogge M. P., Caldwell J. H., Ingram D. R., Green C. E., Geselbracht M. J. and Siegrist T. (1998) A New Synthetic Route to Pseudo-Brookite-Type CaTi₂O₄. *J. Solid State Chem.* **141**, 338–342.
6. Sugano S., Tanabe Y., Tsujikawa I. (1958) Absorption Spectra of Cr³⁺ in Al₂O₃. *J. Phys. Soc. Japan.* **13** (195), 880-899.

Ivanova M.V.¹, Bobrov A.V.^{1,2} Phase relations in mantle rocks at the lunar lower mantle/core boundary: evidence from experiments

¹ Vernadsky Institute of Geochemistry and Analytical Chemistry RAS, ² Lomonosov Moscow State University, Faculty of Geology, mv.iva.nova@yandex.ru

Abstract. According to the data of the Lunar Laser Ranging and the GRAIL (Gravity Recovery and Interior Laboratory) mission, a partially molten zone may be located at the base of the lunar mantle at the boundary with the outer core. This 150-200-km thick zone is presumably located at a depth of ~1200 km and is enriched in FeO and TiO₂ compared to the surrounding mantle. In this paper, based on the experimental study of the CaO-FeO-MgO-Al₂O₃-SiO₂-TiO₂ (CFMASTI) system modeling the substance of the lower mantle layer of the Moon in contact with the liquid core, the main features of phase relations in the subliquidus and subsolidus parts of the system with a high titanium content (10 wt.%) at temperatures of 1000-1600 °C and a fixed pressure of 4.5 GPa were revealed. The resulting phase association includes: olivine, enstatite, diopside, garnet, rutile, ilmenite and melt. The dependences of phase relations on temperatures are determined. The results of experimental studies confirm the probability of partial melting of the matter in the temperature range of 1450-1600°C at depths of ~1200-1400 km.

Keywords: Moon, phase relations, mantle, experiment

One of the main problems of geophysics and geochemistry of the Moon is the problem of studying its deepest parts. A special place in these studies is occupied by experimental methods related to the

physicochemical modeling of endogenous processes and the detailed study of phase associations formed under high pressures and temperatures. In recent years, the reinterpretation of the Apollo program seismic experiment (1969-1972) results, provided by the Apollo Lunar Surface Experiments Package (ALSEP), together with the Lunar Laser Ranging (LLR) data and the Gravity Recovery and Interior Laboratory (GRAIL) mission data, resulted in discovery of a partially molten layer in the lower lunar mantle at the boundary with the core (Kronrod et al., 2015; Khan et al., 2014; Weber et al., 2011). The presence of such layer imposes significant restrictions to the models of the internal structure of the Moon and the lunar thermochemical evolution. Therefore, the experimental verification of the hypothesis of the likely presence of a melt in the transition zone, as well as the establishment of the correspondence of the assumed phase associations to those obtained in the experiment, are extremely important for improving theoretical knowledge about the Earth's satellite interior.

To establish phase relations in a system modeling the substance of the lower-mantle layer of the Moon in contact with the liquid core, we studied a simplified CaO-FeO-MgO-Al₂O₃-SiO₂-TiO₂ (CFMASTi) model system at a fixed pressure of 4.5 GPa and temperatures of 1000-1600°C.

The experiments were carried out in a toroidal high-pressure apparatus of the “anvil with a hole” type (NL-13T) at the Vernadsky Institute of Geochemistry and Analytical Chemistry of the Russian Academy of Sciences. For the experiments, a cell made of a pressed mixture of MgO and BN in a ratio of 3:1 was used, with a working volume of 0.1-0.15 cm³ and a diameter of 30 mm (hole diameter of 13 mm). The sample was loaded into a cylindrical cavity of a 2.5 × 2.5 mm graphite heater, which, in turn, was placed in a solid-phase cell. The pressure

calibration was carried out at room temperature and is based on a change in the electrical resistance of the bismuth wire during reference phase transitions in bismuth at 2.55 (Bi I – Bi II); 2.7 (Bi II – Bi III); 7.7 (Bi III – Bi V) GPa, respectively. Temperature calibration was performed using thermocouples Pt₇₀Rh₃₀/Pt₉₄Rh₆ and an assessment of the temperature dependence on the electric heating power. The error of maintaining and measuring the temperature for the central part of the sample is ±10°C (Sirotkina et al., 2016).

Analysis of samples collected during the Apollo mission showed that only the most titanium-rich melts will be neutrally buoyant in relation to the lunar mantle (Parker et al., 2012). At the same time, the presence of high-titanium phases, such as ilmenite, may contribute to a decrease in the melting temperature of the substrate at depths of 1200-1400 km. Therefore, in this paper a simplified six-component composition was chosen, obtained as a result of inversion of geophysical data taking into account the equations of phase equilibria (Khan et al., 2014), corresponding to the substance of the lower layer of the Moon's mantle at the boundary with the core and following the requirement of generating melts of sufficient density. It is distinguished from other models of the transition layer by an increased content of TiO₂ and understated contents of Al₂O₃, SiO₂. Powdered chemically pure oxides (wt.%) were used as starting materials for the specified compositions of the system: 40% SiO₂; 10% TiO₂; 2% Al₂O₃; 14% FeO; 30% MgO; 4% CaO.

In this work, 4 series of experiments were conducted for each temperature. The experimental conditions at a pressure of 4.5 GPa in the temperature range 1000-1600°C and the obtained phase associations are presented in Table 1.

Table 1. Experimental conditions and phase associations at temperatures of 1000-1600°C and a pressure of 4.5 GPa in the CFMASTi system. The bulk contents of the phases are indicated in parentheses.

Sample №	T, °C	Phase association (vol.%)
165	1000	Ol(22%)+Opx(45%)+Cpx(20%)+Rt(10%)+FeO(3%)
166	1100	Ol(21%)+Opx(43%)+Cpx(19%)+Grt(4%)+Rt(10%)+FeO(3%)
147	1200	Ol(27%)+Opx(44%)+Cpx(8%)+Grt(8%)+Rt(6%)+Ilm(7%)
163	1300	Ol(28%)+Opx(44%)+Cpx(6%)+Grt(7%)+Rt(6%)+Ilm(9%)
167	1400	Ol(29%)+Opx(43%)+Cpx(4%)+Grt(9%)+Rt(6%)+Ilm(9%)
161	1500	Ol(26%)+Opx(46%)+Cpx(3%)+Grt(6%)+Rt(4%)+Ilm(4%)+L(11%)
162	1600	Ol(29%)+Opx(46%)+Grt(4%)+Rt(1%)+Ilm(7%)+L(13%)

Experiments at temperatures of 1000-1100°C are characterized by a fine-grained loose aggregate composed of diopside, enstatite and olivine. Subhedral rutile grains up to 80 microns in size are abundant. There are also single grains of garnets. Experimental samples obtained at 1200°C are

distinguished by the presence of ilmenite (Fig. 1, a). It forms both independent grains and rims around rutile. Olivine and enstatite grains become euhedral and large. The morphology of samples obtained at a temperature of 1300°C differs markedly from that at lower temperatures by the larger size of minerals,

including ore, and an increase in the proportion of ilmenite (Fig. 1, b). Rare garnets are close to isometric and reach 50 microns. With an increase in the temperature of the experiments to 1400°C, the proportions of garnet and olivine increase slightly. Diopside is found only as small inclusions (about 2 microns) in matrix and garnets. At 1500°C, the proportions of minerals are generally preserved, but a

change in the structure of the samples is observed. An interstitial fine-grained aggregate of skeletal crystals appears, which has been interpreted as a quenched melt represented by ilmenite and pyroxenes (Fig. 1, c). An increase in temperature to 1600°C leads to the disappearance of clinopyroxene in the products of experiments and an increase in the proportion of melt (Fig. 1, d).

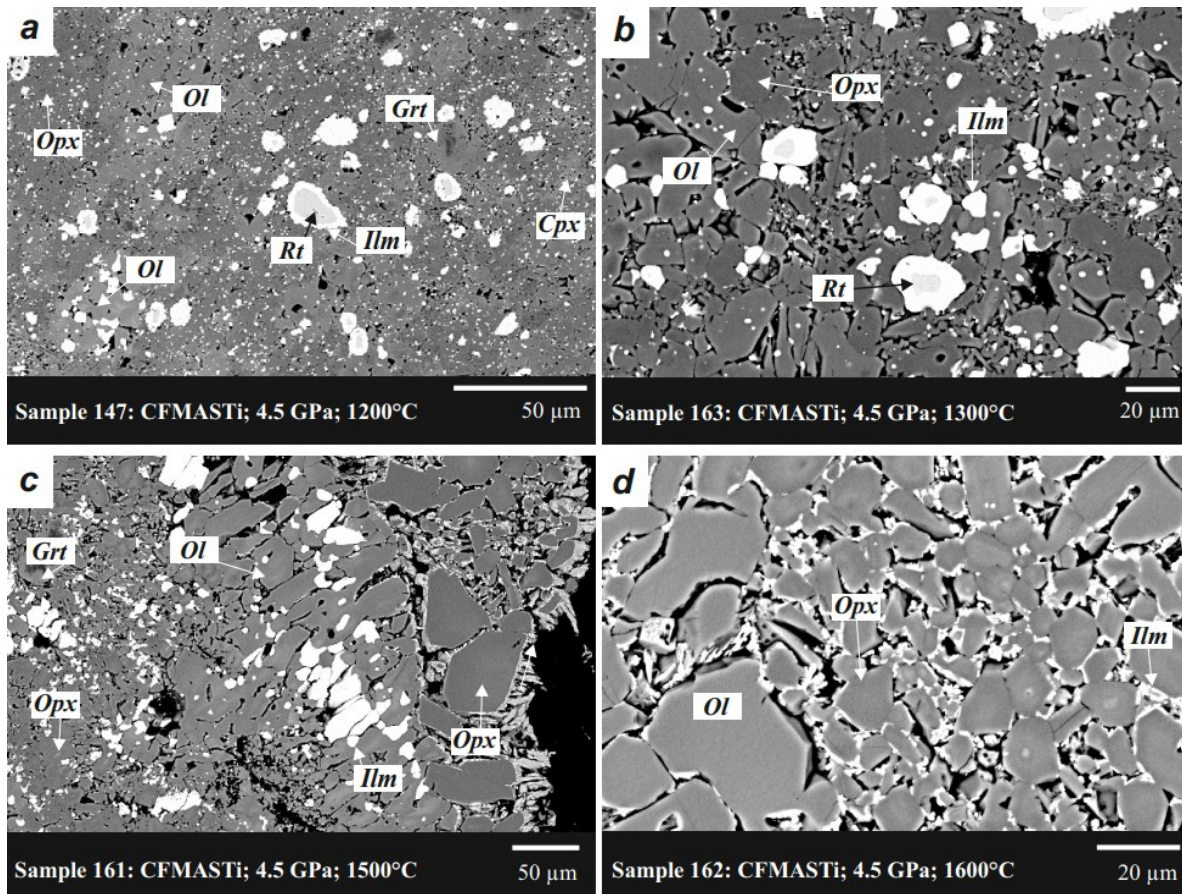


Fig. 1. BSE images of run products obtained at 4.5 GPa and 1200-1600 °C.

The Mg# of clinopyroxenes practically does not correlate with temperature conditions, while for orthopyroxenes it decreases with increasing temperature. The TiO₂ content in pyroxenes tends to increase with increasing temperature, but does not exceed 0.89 wt.% in orthopyroxene and 0.43 wt.% in clinopyroxene. Based on the inverse dependence of TiO₂ contents on SiO₂ in pyroxenes, we suggest the isomorphic substitution of silicon with titanium in the tetrahedral site T. The inverse relationships between the contents of Al₂O₃ and MgO, Al₂O₃ and SiO₂ have also been established, which, together with an increase in alumina concentrations against the background of an increase in temperature, indicates the Tschermak type of substitution according to the scheme: Al(M1) + Al(T) ↔ Mg(M1) + Si(T).

The garnets synthesized in the system are characterized by an excess of silica, which reaches

3.1 formula units and, accordingly, belong to the majoritic type (Gasparik, 2002). The concentrations of aluminum in garnets reach 25.41 wt.% Al₂O₃, iron – 13.56 wt.% FeO, and magnesium – 18.96 wt.% MgO. At the same time, garnets in low-temperature experiments, at 1100°C, have the highest concentrations of CaO (up to 11.48 wt.%), which are not achieved at higher temperatures. Titanium contents vary within 1-3 wt.% TiO₂ and slightly increase with temperature, as do CaO concentrations.

Olivine has wide compositional variations from Fo60 to Fo90. On average, Mg# decreases slightly with increasing temperature. The CaO concentration does not exceed 0.15 wt.% and slightly increases from low-temperature to high-temperature experiments. An isomorphism of Mg²⁺ ↔ Ca²⁺ at site M2 is assumed. TiO₂ contents reach 4.31 wt.% at 1000-1100°C, but dramatically decrease at 1200°C,

with the appearance of ilmenite in the products of experiments. According to the experimental and natural data (Matrosova et al., 2021) the presence of titanium is not characteristic of olivine, therefore, in the olivines obtained in this work under the low-temperature conditions, the admixture of this element is apparently associated with the smallest inclusions in the central parts of olivine grains. At temperatures above 1200°C, the TiO₂ contents do not exceed 0.5 wt.%. The aluminum contents, as well as calcium, are extremely low and amount to less than 0.12 wt.%, but do not show an obvious temperature dependence.

The compositions of ore minerals, such as rutile and ilmenite, are quite stable and practically independent on temperature. They are the main hosts for titanium. There is also an isomorphic substitution

of Fe²⁺ ↔ Mg²⁺ in ilmenite, while the MgO content reaches 14 wt.%. In this regard, it may be identified as picroilmenite, which in terrestrial conditions is an indicator mineral of kimberlite.

The melt in experiments at 4.5 GPa and 1500-1600°C in the “dry” CFMASTi system is not a tempered homogeneous glass typical of more acidic compositions, but is a more complex, multiphase mixture of a quenching nature. It is fixed by the dendritic texture in interstitials. The composition of the melt was estimated by carrying out mass balance calculations (Ariskin et al., 2000) and is presented in Table 2. Modal mineral contents are established in the ImageJ and CT-An programs based on images of experimental samples in reflected electrons.

Table 2. The calculated melt composition in the CFMASTi system at 4.5 GPa and 1500-1600°C.

Components (wt.%)	SiO ₂	TiO ₂	Al ₂ O ₃	FeO	MgO	CaO
1500 °C	4	30	2	28	17	18
1600 °C	12	34	3	13	14	23

Thus, the results of this study confirm the probability of partial melting of the substrate in the temperature range of 1450-1600°C at depths of about 1200-1400 km. The degree and temperature of melting are in good agreement with the calculated and experimental literature data (Antonangeli et al., 2015; Mallik et al., 2019; Parker et al., 2012; Weber et al., 2011), and the mineral association corresponds to the predicted one in the models (Kronrod et al., 2011; Kuskov et al., 2019; Khan et al., 2014). It is important to note the presence of garnet and calcium pyroxene in the obtained experimental samples. Garnet occurs in the experimental products to temperatures of about 1550°C, diopside – up to 1500°C. In other experimental studies, where the composition of the partially molten layer is approximated by the composition of Fe-Ti cumulates or their mixture with the mantle matter of the Moon after 50% crystallization of the lunar magmatic ocean in a ratio of 1:1 (Mallik et al., 2019), garnet and calcium pyroxene are detected only up to 1400°C. Nevertheless, according to the latest experimental data (Jing et al., 2022), garnet in the lunar mantle is stable at pressures greater than 3 GPa and temperatures less than 1700°C, and calcium pyroxene is stable at pressures greater than 3 GPa and temperatures up to 1600 °C, which is confirmed by the current study.

References

- Antonangeli D., Morard G., Schmerr N.C., Komabayashi T., Krisch M., Fiquet G., Fei Y. Toward a mineral physics reference model for the Moon's core // *PNAS*, 2015, v.112, № 13, pp. 3916-3919.
- Ariskin A.A., Barmina G.S. Modeling of phase equilibria during crystallization of basalt magmas // *M: Science*, 2000, 363 p.
- Gasparik T. Experimental investigation of the origin of majoritic garnet inclusions in diamonds // *Physics and Chemistry of Minerals*, 2002, v.29, pp. 170-180.
- Jing J.J., Lin Y., Knibbe J.S., Wim van Westrenen. Garnet stability in the deep lunar mantle: Constraints on the physics and chemistry of the interior of the Moon // *Earth and Planetary Science Letters*, 2022, v.584, №117491, pp. 1-13.
- Khan A., Connolly J.A.D., Pommier A., Noir J. Geophysical evidence for melt in the deep lunar interior and implications for lunar evolution // *Journal of Geophysical Research Planets*, 2014, v.119, pp. 2197-2221.
- Kronrod E.V., Kronrod V.A., Kuskov O.L. Restrictions on the thermal regime and the uranium content in the lunar substance for a model of the magmatic ocean with conditions of partial melting of mantle matter in the vicinity of the core // *Mechanics, Management and Informatics*, 2015, v.7, №3, pp. 89-101.
- Kronrod V.A., Kuskov O.L. Modeling of the chemical composition and size of the Moon's core by inversion of seismic and gravitational data // *Physics of the Earth*, 2011, №8, pp. 62-80.
- Kuskov O.L., Kronrod E.V., Kronrod V.A. Influence of the thermal state on the chemical composition of the

-
- mantle and the size of the Moon's core // *Geochemistry*, 2019, v.64, №6, pp. 567-584.
- Mallik A., Ejaz T., Shcheka S., Garapic G. A petrologic study on the effect of mantle overturn: Implications for evolution of the lunar interior // *Geochimica et Cosmochimica Acta*, 2019, v.250, pp. 238-250.
- Matrosova E.A., Bobrov A.V., Bindi L., Pushcharovsky D.Y. Titanium minerals and their associations in the Earth's mantle: a review of natural and experimental data // *Geochemistry*, 2021, v.66, №8, pp. 675-693.
- Parker M.V., Sanloup C., Sator N., Guillot B., Tronche E.J., Perrillat J.P., Mezouar M., Rai N., Westrenen W.V. Neutral buoyancy of titanium-rich melts in the deep lunar interior // *Nature Geoscience*, 2012, v.5, pp. 186-189.
- Sirotkina E.A., Bobrov A.V., Kargaltsev A.A., Ignatiev Yu.A., Kadik A.A. Influence of low aluminum concentrations on the composition and crystallization conditions of majorite–knorringite garnets: experiment at 7.0 GPa and 1500-1700°C // *Geochemistry*, 2016, №7, pp. 596-606.
- Weber R.C., Lin P., Garnero E.J., Williams Q., Lognonné P. Seismic detection of the lunar core // *Science*, 2011, v.331, pp. 309-312.